

Frequent new particle formation at remote sites in the temperate/boreal forest of North America

Meinrat O. Andreae^{1,2,3}, Tracey W. Andreae¹, Florian Ditas^{1,4}, and Christopher Pöhlker¹

Deleted: and

¹Max Planck Institute for Chemistry, Mainz, Germany

²Scripps Institution of Oceanography, La Jolla, California, USA

³Department of Geology and Geophysics, King Saud University, Riyadh, Saudi Arabia

⁴Hessian Agency for Nature Conservation, Environment and Geology, Wiesbaden, Germany

Correspondence to: Meinrat O. Andreae (m.andreae@mpic.de)

Abstract. The frequency and intensity of new particle formation (NPF) over remote forest regions in the temperate and boreal zones, and thus the importance of NPF for the aerosol budget and life cycle in the pristine atmosphere, remains controversial. Whereas NPF has been shown to occur relatively frequently at several sites in Scandinavia, it was found to be nearly absent at a mid-continental site in Siberia. To explore this issue further, we made measurements of aerosol size distributions between 10 and 420 nm diameter at two remote sites in the transition region between temperate and boreal forest in British Columbia, Canada. The measurements covered 23 days during the month of June 2019, at the time when NPF typically reaches its seasonal maximum in remote mid-latitude regions. These are the first such measurements in a near-pristine region on the North American continent. Although the sites were only 150 km apart, there were clear differences in NPF frequency and intensity between them. At the Eagle Lake site, NPF occurred daily and nucleation mode particle concentrations reached above 5000 cm⁻³. In contrast, at the Nazko River site, there were only 6 NPF events in 11 days and nucleation mode particle concentrations reached only about 800 cm⁻³. The reasons for this difference could not be conclusively resolved with the available data; they may include air mass origins, pre-existing aerosols, and the density and type of forest cover in the surrounding regions. In contrast to observations in other temperate/boreal environments, we found that NPF at our sites occurred at nighttime just as frequently as during daytime. Together with the lack of identifiable sources of H₂SO₄ precursor species in the fetch region of our sites, this suggests that nucleation of extremely-low-volatility organics was the predominant NPF mechanism. Our results indicate that extended measurement campaigns with a more comprehensive set of instrumentation in the remote forest regions of North America to investigate the role of NPF are essential for a deeper scientific understanding of this important process and its role in the global aerosol budget.

Deleted: dramatic

Deleted: suggest

Deleted: with a more comprehensive set of instrumentation

1 Introduction

Uncertainty regarding the magnitude of aerosol direct and indirect radiative effects is the largest contributor to the persistent uncertainty of net radiative forcing, which drives global and regional climate change (Boucher et al., 2013; Seinfeld et al., 2016; Bellouin et al., 2020; Naik et al., 2021). Since by definition this forcing is the difference between present-day and pre-industrial radiative effects, both need to be known accurately to assess present-day forcing and prognosticate future forcings. Because of the strong non-linearity of the aerosol effects on cloud microphysics and precipitation, this applies in particular to the aerosol indirect effects, also referred to as aerosol-cloud interactions (ACI) (Twomey et al., 1984; Rosenfeld et al., 2008; Carslaw et al., 2013; Carslaw et al., 2017). Adding the same amount of pollution aerosol to a pre-industrial atmosphere with very low initial particle concentration would cause a much greater radiative forcing than

adding the same amount to an atmosphere with a higher pre-industrial background (Carslaw et al., 2013; Gordon et al., 2016; Hamilton et al., 2018).

45 Because the ACI are driven by the microphysical perturbations of cloud properties by aerosols, they are a function of the number concentration of cloud condensation nuclei (CCN), i.e., the subset of aerosol particles that can nucleate cloud droplets. It is thus essential to understand the sources and lifecycles of this particle class in both polluted and pristine atmospheres. While some CCN are the result of physical processes that directly release particles into the atmosphere, e.g., seaspray and mineral dust, a large and possibly dominant fraction of CCN is the result of secondary production of particles
50 from the condensation of trace vapors. Models suggest that around 40-70% of global CCN originate from nucleation of gaseous compounds and subsequent growth of the nucleated embryos into aerosol particles, a process called new particle formation (NPF) (Merikanto et al., 2009; Wang and Penner, 2009; Yu and Luo, 2009; Zhang et al., 2012; Dunne et al., 2016; Gordon et al., 2017; Kerminen et al., 2018). The importance of NPF for the global CCN budget may be higher in pristine than anthropogenically perturbed atmospheres: Gordon et al. (2017) estimated a contribution by NPF of 67% of
55 CCN for the preindustrial atmosphere in contrast to 54% at the present day.

Under present-day conditions, sulfuric acid (H_2SO_4) driven pathways are considered to dominate daytime nucleation, based on laboratory studies (Sipilä et al., 2010) and field measurements at numerous sites (Kerminen et al., 2018; Nieminen et al., 2018), e.g., Hyytiälä, Finland (Ehn et al., 2010; Kulmala et al., 2013), the high Arctic (Giamarelou et al., 2016), and marine environments (Brean et al., 2021; Zheng et al., 2021). In these pathways, gaseous H_2SO_4 is required
60 to form the initial clusters, which are stabilized synergistically by NH_3 , amines, and organics, particularly highly oxidized molecules (HOMs) (Zhang et al., 2012; Kulmala et al., 2013; Schobesberger et al., 2013; Riccobono et al., 2014; Dal Maso et al., 2016; Kürten et al., 2018; Lehtipalo et al., 2018). In addition to these sulfuric acid driven pathways, models and laboratory studies suggest that pure organic nucleation, possibly ion-induced, may be a significant source of new particles in present-day pristine and pre-industrial atmospheres (Jokinen et al., 2015; Gordon et al., 2016; Kirkby et al.,
65 2016; Gordon et al., 2017; Zhu and Penner, 2019). This has been supported by observations at some remote upper tropospheric sites, e.g., in the Himalayas (Bianchi et al., 2021) and the Bolivian Andes (Rose et al., 2015).

In contrast to H_2SO_4 driven NPF, which most commonly happens in the first half of the day, pure organic nucleation can also result from the nighttime oxidation of biogenic volatile organic compounds (BVOCs) by ozone or by autoxidation to form highly oxidized molecules (HOMs) with extremely low volatility. Nighttime nucleation has been observed
70 to occur frequently in some environments with low condensation sinks (Vehkamäki et al., 2004; Lee et al., 2008; Suni et al., 2008). HOM dimer concentrations have their maxima during the night (Sulo et al., 2021), and HOMs from monoterpene oxidation have been observed to drive nighttime nucleation in springtime at Hyytiälä (Rose et al., 2018). Laboratory studies and quantum chemical calculations demonstrate the important role of monoterpene oxidation products for nighttime nucleation (Ortega et al., 2012; Bianchi et al., 2019). Once new particles with diameters of a few nm have
75 formed, they can grow by condensation of additional sulfates and organics. Particle growth at sites without high pollution levels is dominated by condensation of organics, mostly from the oxidation of biogenic VOCs (Riipinen et al., 2012; Ehn et al., 2014; Dal Maso et al., 2016; Tröstl et al., 2016; Bianchi et al., 2019).

Reviews of the worldwide distribution of NPF events have shown them to occur in all types of environments, from very remote to highly polluted (Kerminen et al., 2018; Nieminen et al., 2018; Bousiotis et al., 2021). Generally, NPF frequencies are highest at pollution-impacted sites, e.g., the Po Valley (Kontkanen et al., 2016), Mexico City (Dunn et al., 2004),
80 and Beijing (Yan et al., 2021). However, NPF has also been shown to occur quite frequently at rural sites, for example Hyytiälä, Finland, where the highest frequency is observed in spring with 47% of days being NPF days (Dada et al., 2018; Nieminen et al., 2018). The role that anthropogenic emissions play at these rural and some remote sites is still unclear. In a study at a remote site in northern Finland, Kyrö et al. (2014) showed that the frequency of NPF events declined with

85 decreasing SO₂ emissions from a smelter in the region. Similarly, NPF was found to occur fairly frequently at two Siberian
sites located in the boreal forest (Dal Maso et al., 2008), but the proximity of high-emitting urban and industrial regions
(Tomsk and Irkutsk) makes the interpretation of these results problematic. This also applies to the few NPF studies in
North America at sites in the temperate forest zone. At Egbert, Ontario, Canada, nucleation occurred frequently, but SO₂
90 concentrations in the range of 1-3 ppb during event days are clear evidence of substantial anthropogenic input even under
relatively clean conditions for this site (Pierce et al., 2014). Similarly, SO₂ concentrations of 0.3 to 1 ppb indicate a
significant anthropogenic influence at an isoprene-dominated site in the Ozark Mountains, Missouri, where frequent and
intense NPF was observed (Yu et al., 2014). At Whistler, British Columbia, there was evidence for NPF on five days
during a period of atmospheric high pressure and elevated temperatures, but the presence of SO₂ in the range of 0.05 to
0.1 ppb suggests that anthropogenic emissions also played a role here (Pierce et al., 2012).

95 Unfortunately, there are very few NPF studies at truly remote continental sites, in part because it is quite difficult to find
sites with near-pristine conditions on the continents (Andreae, 2007). The sites classified as remote in Nieminen et al.
(2018) are all in regions where significant anthropogenic pollution can be expected, at least much of the time, e.g., Fi-
nokalia, Greece, and Mt. Waliguan, China. In contrast to these “remote” sites, where annual median NPF frequencies
around 20% have been observed, NPF was found to be very rare during multi-year observations at very remote sites in
100 Central Siberia (Wiedensohler et al., 2019; Uusitalo et al., 2021) and almost absent in the central Amazon Basin (Andreae
et al., 2015; Rizzo et al., 2018; Wimmer et al., 2018; Franco et al., 2021). In the Amazon, NPF was, however, detected
occasionally at sites affected by the pollution plume from Manaus, indicating the effect of even quite small amounts of
anthropogenic inputs on NPF (Rizzo et al., 2018; Wimmer et al., 2018).

The stark contrast between the observations of frequent NPF at the Scandinavian rural and remote sites, and its near-
105 absence at our remote Siberian and Amazon sites prompted us to ask the question, whether NPF in the planetary boundary
layer over vegetated land surfaces would only occur in the presence of at least a minor amount of recent anthropogenic
SO₂ inputs, or if it could also happen in a truly pristine environment. In particular, we were interested to address this
question in an area comparable to the temperate-to-boreal forest environment that has been shown to be a prolific source
of new particles in Northern Europe. Based on maps of aerosol optical depth (e.g., Huneus et al., 2012), vegetation types,
110 topography, and potential anthropogenic sources we identified the interior of British Columbia, Canada, as a suitable
region for a pilot study. Measurements in this region seemed especially important in view of the fact that no studies on
NPF had been conducted at any near-pristine site in North America.

The objectives of our study were (1) to determine whether NPF in a pristine subboreal forest environment was frequent,
like at the Scandinavian sites, or almost non-existent, like at the Central Siberian sites, (2) elucidate the role of anthropo-
115 genic SO₂ emissions in NPF by making measurements in a region where such emissions were likely to be negligible, (3)
examine the hypothesis that nighttime NPF would be frequent in the absence of significant sources of H₂SO₄ vapor, and
(4) examine whether the results from such a limited pilot study would warrant future, more comprehensive and extended
studies. Here, we present the results of measurements of aerosol size distributions in the range between 10 and 420 nm
diameter at two remote sites in the transition region between temperate and boreal forest in British Columbia, Canada,
120 collected over 23 days during the month of June 2019. From these measurements, we derived estimates of NPF frequency,
particle growth rate, and condensation sink.

2 Methods

2.1 Measurement sites

Our measurements were conducted at two remote locations in the Fraser River basin of British Columbia, Canada (Fig. 1a). The basin lies between the Coast Mountains to the West and the Rocky Mountains to the East and has a generally gentle topography, dominant coniferous forest cover, and very low population density (<0.5 km⁻²). The few larger towns are along the Fraser River and Highway 97, far downwind (70 to 160 km) of our sites during the prevailing westerly winds. Backtrajectory analysis showed that the sampled airmasses did not contact this inhabited region.

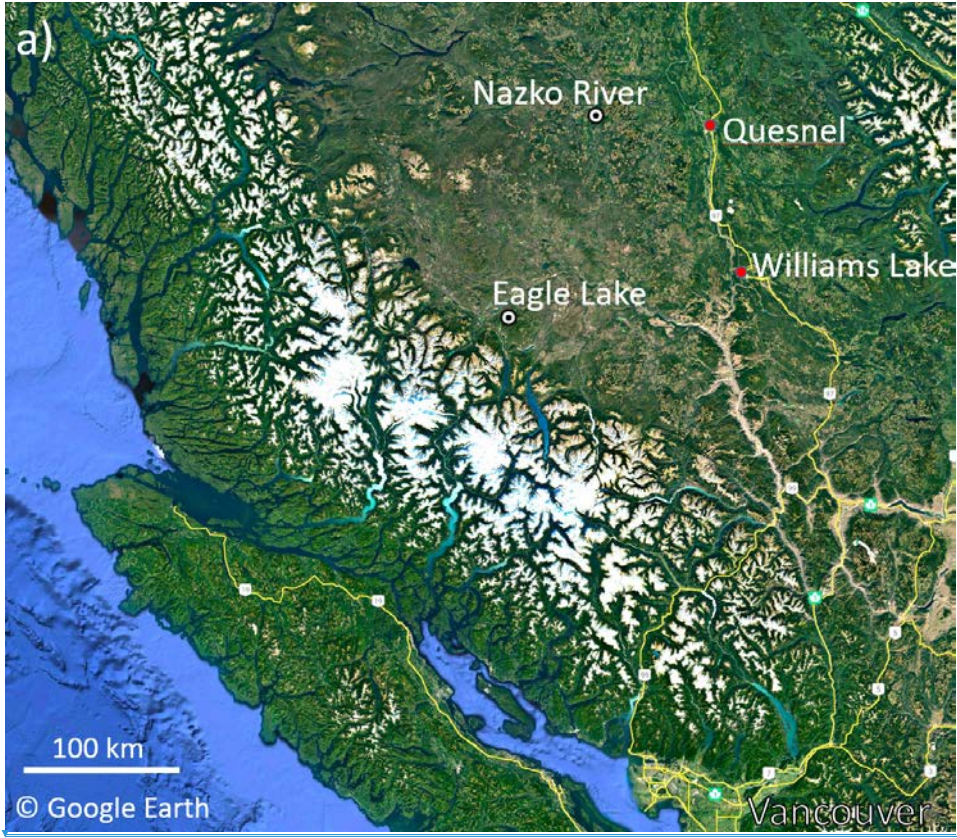
2.1.1 Eagle Lake

The Eagle Lake (EL) site (51.90 °N, 124.38 °W, 1066 m a.s.l.) is on a small, isolated ranch surrounded by large tracts of predominantly evergreen forest (Fig. 1b). Evergreen needleleaf closed and open forest together make up 85% of land cover in the fetch region, with the remainder dominated by herbaceous vegetation and bare/sparse plant cover. Visual examination showed a low abundance of aspen in the region. A small lake (Eagle Lake) lies northwest of the site. A few cabins are located about 4 km away on the other side of the lake. Access is by a rough road that dead-ends at the ranch. The instrumentation was deployed in a small cabin west of the ranch house. Electric power was provided by a small hydroelectric generator. The aerosol inlet was located about 2 m above ground level, and the sample air was brought into the cabin by ca. 2 m of 6.25 mm OD copper tubing. Tests comparing measurements with and without the inlet tubing at times with a pronounced nucleation mode showed no detectable particle loss. The air was sampled without the use of a dryer.

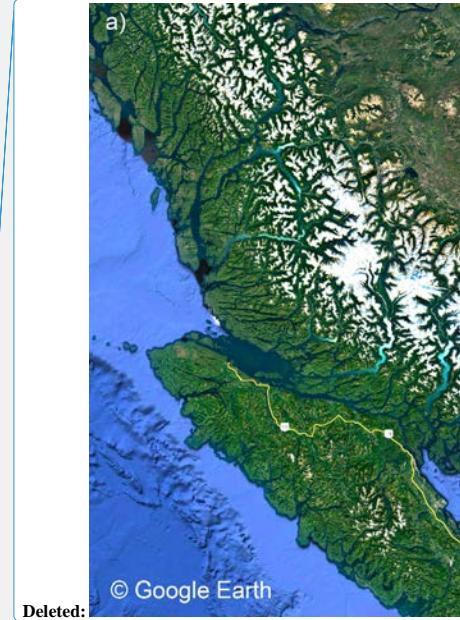
Deleted: The instrumentation was deployed in a small cabin west of the ranch house.

Moved down [2]: Access is by a rough road that dead-ends at the ranch.

Moved (insertion) [2]



145



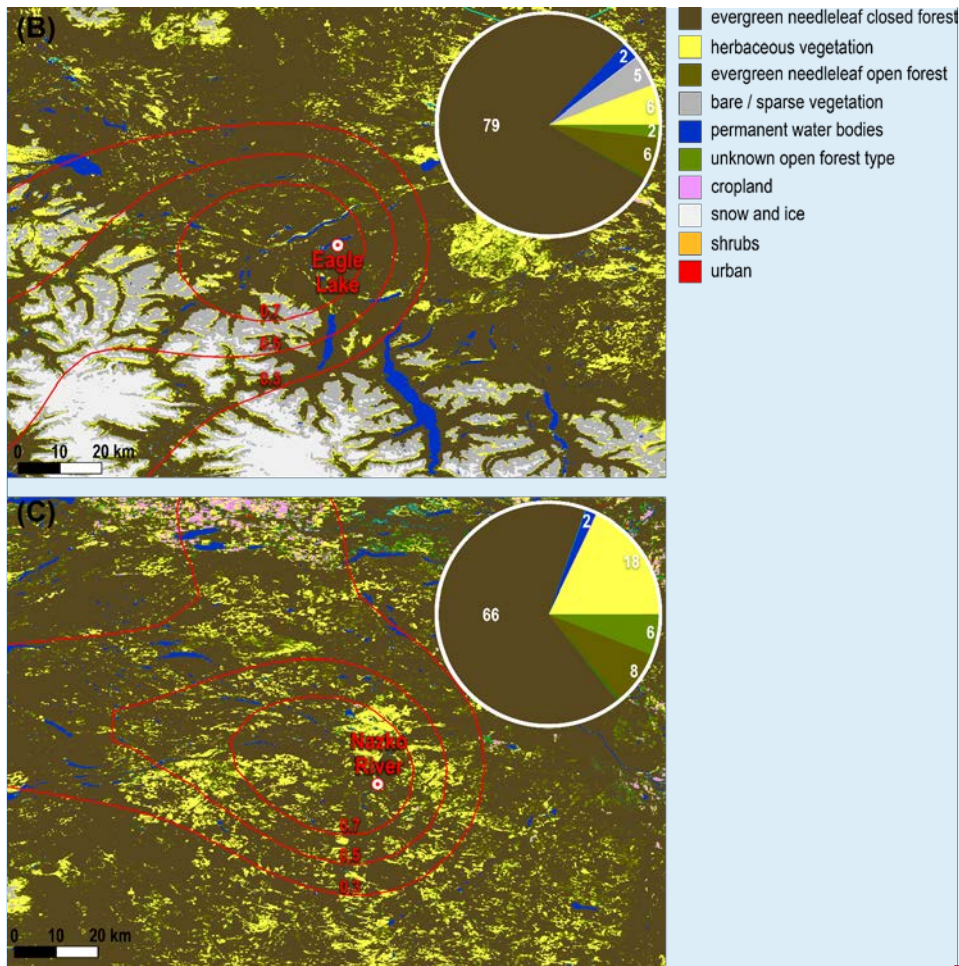


Fig. 1: a) Overview map of the sampling area (Map base © Google Earth). b) and c) Land cover maps with backward trajectory densities, represented by 0.3, 0.5 and 0.7 contour lines, for Eagle Lake and Nazko River. The pie charts in (b) and (c) represent the land cover fractions (in %) for the areas within the 0.7 contour line.

2.1.2 Nazko River

The Nazko River (NR) site consists of a small isolated cabin (53.08 °N, 123.56 °W, 840 m a.s.l.) on the western bank of the Nazko River (Fig. 1c). The fetch region is characterized by a patchwork of evergreen forest and open areas with regrowth of small pines, abundant small and medium-sized aspen, and weedy vegetation. The area covered by evergreen needleleaf forest in the fetch region represents 74% of land cover, whereas the area classified as unknown open forest (6%) and herbaceous vegetation (18%), much of which includes aspen, covers a much larger fraction at NR than at EL. A small gravel road runs about 200 m west of the site, with a traffic volume of a few tens of vehicles per day. No response from the few passing cars could be detected in the data. There is no human habitation for at least 80 km in the upwind fetch of the site. Electricity was provided by line power. The instrument was located in a small shed upwind of the cabin, with an inlet layout similar to that at EL.

Commented [MOA1]: Fig 1b and 1c to be replaced by land-cover maps from Christopher



Deleted:



Deleted:

Deleted: B

Deleted: detailed view of the land cover in the area surrounding the Eagle Lake site. c) detailed view of the land cover in the area surrounding the Nazko River site

Deleted: (Map base © Google Earth)

Deleted: .

170 **2.2 Instrumentation**

The measurements of aerosol number size distribution were made with a Nanoscan 3910 SMPS Particle Sizer (TSI Inc., Shoreview, Minn., USA). The Nanoscan 3910 uses a unipolar corona charger, a radial differential mobility analyzer, and an isopropanol-based Condensation Particle Counter (CPC). It measures nanoparticle size distributions from 10 to 420 nm (13 channels) in one-minute intervals. The response is linear between 10^2 and 10^6 cm^{-3} , and the sizing accuracy is better than 8%. Based on the manufacturer, particle diameters and concentrations agree to within 5% with measurements made using a TSI SPMS 3936 particle sizer, and the reproducibility for median particle diameter and total concentration are 1.1% and 2.7%, respectively (TSI Inc. Application Note NANOSCAN-002). An independent study showed similar agreement, with deviations of particle size $\leq 4\%$ and concentration $\leq 10\%$ (Vo et al., 2018). The instrument was calibrated by the manufacturer before the field deployment. For the calculation of aerosol mass concentrations, the density of 1.2 g cm^{-3} specified by the manufacturer was used. Concentration data are reported relative to ambient temperature and pressure.

185 **2.3 Meteorological information**

Meteorological data were obtained from the NARR (North American Regional Reanalysis) database using the NOAA - READY (National Ocean and Atmospheric Administration - Real-time Environmental Applications and Display sYstem) tool (Rolph et al., 2017). The NARR data is available on a 3-hourly, 32-km grid. The NARR project is an extension of the NCEP Global Reanalysis, which is run over the North American Region. The NARR model uses the very high resolution NCEP Eta Model (32-km/45 layer) together with the Regional Data Assimilation System (RDAS), which assimilates precipitation along with other variables. Backward trajectories (BT) were computed using the NOAA Hybrid Single-Particle Lagrangian Integrated Trajectory model (HYSPLIT) with meteorological input data from the Global Data Assimilation System (GDAS, 1° resolution) (Stein et al., 2015).

190 **2.4 Land cover and footprint analysis**

For the land cover and footprint analysis, BTs were generated with HYSPLIT using the matrix option with nine individual BTs within areas of about 35 km x 35 km centered around the Eagle Lake and Nazko River sites. The matrix option was chosen to obtain a regional instead of a rather localized representation of the air mass history. As meteorological input data, the Global Data Assimilation System (GDAS) output with 0.5° resolution as well as the Global Forecast System (GFS) output with 0.25° resolution were used. As the GFS 0.25° data was only available from 12 June 2019 onwards, the GDAS 0.5° data had to be used before. BTs were generated from 04 June 2019 until 26 June 2019. Their starting height was 100 m and duration was 48 h.

The further analysis steps were conducted in the QGIS software package (version 3.12, QGIS development team, <https://www.qgis.org/>, last access 15 Jan 2022) using the coordinate reference of the World Geodetic System from 1984 (WGS84). For both sites, the individual BT files were merged into density maps and the highest densities were normalized to unity. Subsequently, the 0.7, 0.5 and 0.3 contour lines were calculated. The land cover data for 2019 was obtained from the Copernicus Global Land Service under <https://land.copernicus.eu/global/products/lc> (last access 06 Feb 2021). The land cover fractions (pie charts) were calculated within the 0.7 contour line.

205

Deleted:

2.5 Ancillary aerosol data

Concentrations of seasalt, dust, and black carbon (BC) aerosol for the study region were obtained from the Modern-Era Retrospective analysis for Research and Applications, Version 2 (MERRA-2) data base using the Giovanni online data system (<https://giovanni.gsfc.nasa.gov>).

2.6 Identification of NPF events and calculation of NPF parameters

New particle formation events were identified using the procedure and criteria of Kulmala et al. (2012). The criteria for an NPF event were: (1) a distinct increase of N_{nuc} (particles 10 to 24 nm diameter) concentrations, (2) formation of a new nucleation mode persisting for more than two hours, and (3) growth of the nucleation mode over several hours. The NPF event identification was first performed by an automated routine (Franco et al., 2021) and then verified visually on the basis of the daily surface plots of the time series of the number size distributions and the time evolution of N_{nuc} particles. A few events erroneously flagged as NPF by the automated algorithm were removed.

~~We estimated the condensation sink (CS) at our sites from size distribution data from the Nanoscan and the dust and seasalt concentrations from the MERRA-2 reanalysis, using the equations in Kulmala et al. (2012). The size distribution of dust and seasalt was represented by a single mode at 3.5 μm with a geometric standard deviation of 2.0 (Albani et al., 2014). The CS was completely dominated by the submicron aerosol, with dust and seasalt typically contributing less than 1%. For comparability with other sites, we calculated CS using the diffusion coefficient of H_2SO_4 , although, as will be discussed below, it is more likely that the actual condensing species were organic compounds.~~

We calculated the growth rates (GR) of the newly formed particles based on the method of Kulmala et al. (2012) by fitting modes to the observed size distributions and deriving the time rate of change of the modal diameter during the growth phase of the NPF event.

Given the lower cutoff of our instrument at 10 nm, we were not able to derive an estimate for the actual nucleation rate, J^* . Instead, we calculated the formation rate of particles >10 nm, J_{10} , from the rate of increase of particle number concentrations in the size range 10 – 24 nm during the early part of the NPF events, following the method of Kulmala et al. (2012). We applied the correction for the coagulation sink, using the parameterization given in eq. (7) of that paper to derive the coagulation sink related to the condensation sink.

3 Results and discussion

3.1 Meteorological background

The meteorological conditions at both sites during the study periods are summarized in Figs. 2a and 2b. Overall, conditions at both sites were mostly fair or partly cloudy, with abundant sunshine and occasional light showers. Overcast skies were encountered occasionally, most frequently in the morning or during the passage of showers. An extended period of overcast from 9 to 11 Jun at EL consisted mostly of high thin cloud. Daytime shortwave radiation levels showed mid-day maxima generally between 600 and 900 W m^{-2} .

The passage of a synoptic cycle at EL resulted in dominant low pressure at the beginning and end of the study period, with a high-pressure system in the middle of the period. This resulted in an overall dominance of fairly light (average 3.0 m s^{-1} , range 2.0-6.3 m s^{-1}) southwesterly to northwesterly winds, with a brief period of southeasterly winds when the pressure was falling on 11-12 Jun. Temperatures were initially low at EL, with highs around 10 °C and lows around 5 °C, but increased to highs around 20 °C and lows around 10 °C after the passage of the high pressure system. Relative humidities were in the range of 24-84%, averaging 55%.

Deleted: 4

Formatted: Heading 2

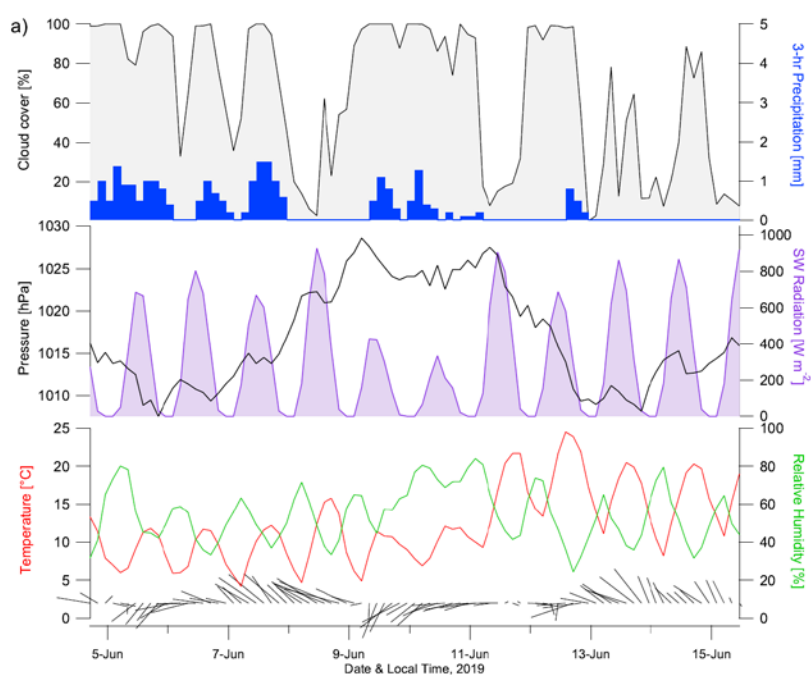
Moved (insertion) [1]

Deleted: CS

Deleted: ¶
¶

250 At NR, winds were predominantly northerly to northwesterly, with a brief period of southwesterly winds on 17 Jun. Wind speeds were slightly higher than at EL (average 3.9 m s^{-1} , range $3.2\text{-}8.5 \text{ m s}^{-1}$). Low temperatures were typically between 5 and $10 \text{ }^\circ\text{C}$ and highs between 13 and $21 \text{ }^\circ\text{C}$, and relative humidities were in the range of 29-93%, averaging 60%, slightly more humid than at EL.

255 [To assess the representativeness of the meteorological conditions during our study, we compared them with the means of the corresponding meteorological parameters for the period 2000 to 2021 in the study region from the MERRA-2 reanalysis for temperature, precipitation, shortwave \(SW\) radiation, and specific humidity, and from MODIS for cloud cover. With the exception of SW radiation, the monthly mean values for June 2019 were within \$\pm 4\%\$ of the long-term averages, and well within 1 standard deviation \(S.D.\) of the mean \(Supplementary Table S1\). Shortwave radiation was 12% \(or 1.6 S.D.\) greater than the long-term average. For a closer examination of the variables most likely to affect NPF, i.e., temperature and SW radiation, we plotted the time series of their daily mean values in June 2019 together with the corresponding time series for the average, standard deviation, and range for the 2000-2021 averages \(Supplemental Fig. S1\). The June 2019 values fluctuate around the long-term average values, with most 2019 values falling within the \$\pm 1\$ S.D. range. We conclude that the meteorological conditions during our study were typical for the season, with no substantial bias that might have affected our results.](#)



265

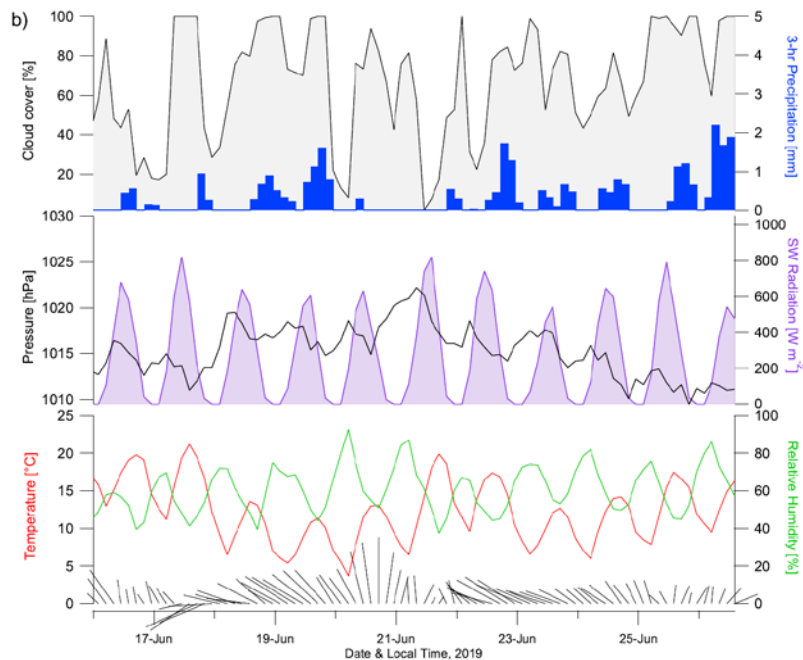


Fig. 2: Meteorograms for the study periods at the a) Eagle Lake and b) Nazko River sites. Wind direction and speed are indicated by barbs at the bottom of the plots. (All data are from the NARR (North American Regional Reanalysis) database.)

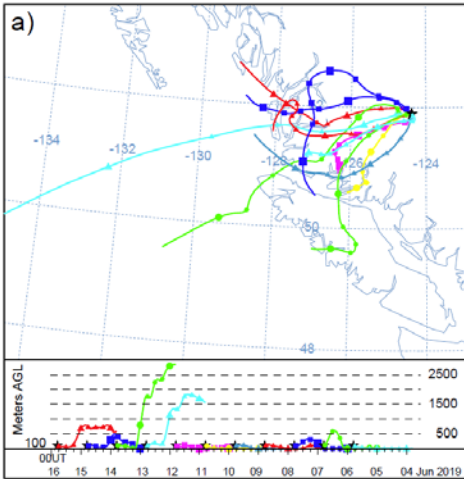
270 **3.2 Airmass history**

We investigated the history of the sampled airmasses using 48-hour and 10-day backtrajectories initialized 100 m above surface level at 12 local time (LT = 19 UTC). The 48-h airmass backtrajectories are shown for the two sites in Figs. 3a and 3b (the 72-h backtrajectories for each individual day are available in the Supplement). All trajectories for the Eagle Lake site had crossed the Pacific coast 22 to 48 hours before arriving at the site and then traveled across the densely forested Coast Range. This fetch area has an extremely low population density and is devoid of any industrial activity. All but two of the trajectories travelled in the boundary layer for at least 48 hours before their arrival. The airmasses arriving on 12 and 13 Jun had not made surface contact with the ocean surface; instead, they arrived from the free troposphere over the Pacific, and descended rapidly after having crossed the Coast Range.

Deleted: initialized 100 m above surface level at 12 local time (LT = 19 UTC)
 Deleted: separate

275

★ Eagle Lake Site: 51.90 N, 124.38 W, Initial height: 100 m AGL



★ Nazko River Site: 53.08 N, 123.56 W, Initial height: 100 m AGL

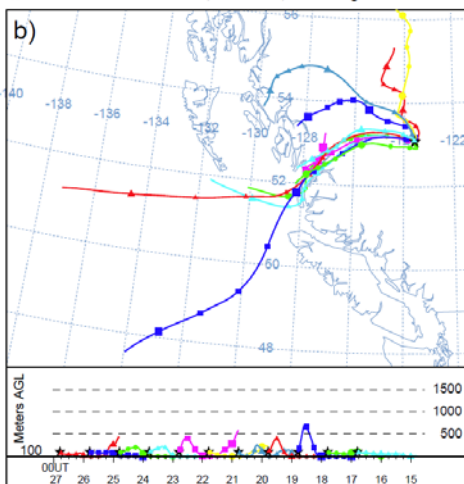


Fig. 3: 48-hour backtrajectories initialized on each sampling day at 1900 UTC at 100 m above ground level at a) Eagle Lake and b) Nazko River.

285

With two exceptions, the airmasses arriving at the Nazko River site also arrived from the Pacific coast, which they had crossed about 14 to 48 hours before arriving at NR. During and after crossing the Coast Range, they remained in the boundary layer for their entire travel. Similar to the fetch at EL, there is no industrial activity and very little human population in this fetch area. Two airmasses arrived from the North and had not made contact with the ocean surface in the last 72 hours. These airmasses originated in an area that had been influenced by the smoke from fires that had been burning for several weeks in northern Alberta, and about 24 h before arriving at NR, they crossed the small municipality of Vanderhoof, which lies 108 km from the site and has a population of about 10,000 persons.

290

In summary, our analysis of the history of the sampled airmasses shows that they had no significant input of anthropogenic emissions for at least 3 days before our measurements. An analysis of 10-day backtrajectories showed that even on this

295 time scale, almost all air masses had remained over the Pacific Ocean, with only a few trajectories crossing over remote regions of British Columbia or Alaska (Supplemental Figs. S2a and S2b).

3.3 Aerosol concentrations and size distributions

300 Figures 4a and 4b show time series of the number concentrations of aerosol particles in the nucleation mode (N_{mic} ; 10 to 24 nm diameter) and across the entire size range covered by the Nanoscan SMPS (N_{420} ; 10 to 420 nm), as well as the aerosol mass concentration in the 10 to 420 nm range (M_{420}) derived from the number spectra by assuming spherical particles with a density of $1.2 \mu\text{g cm}^{-3}$. The corresponding size distributions are shown in Figs. 5a and b. The mass concentrations of dust, seasalt, and BC from the MERRA-2 models are provided in the supplement (Supplemental Figs. S3a and b).

305 The measurements at Eagle Lake indicate an extremely clean atmosphere: The time series plot of aerosol number size distributions (Fig. 5a) is dominated by particles below 100 nm, often with a distinct nucleation mode below 20 nm and a separate Aitken mode between 20 and 80 nm. The accumulation mode tends to be absent or weak, except for a short period on 12 and 13 Jun, when a mode around 100 nm could be interpreted as a more pronounced accumulation mode.

310 The mass concentrations, M_{420} , are very low (Fig. 4a), with an average of 0.73 (range $0.11 - 2.3$) $\mu\text{g m}^{-3}$, ten times lower than the average $\text{PM}_{2.5}$ value of $7.3 \mu\text{g m}^{-3}$ for North America (Mortier et al., 2020). The BC, dust, and seasalt concentrations from MERRA-2 are also very low, at 0.041 ± 0.011 , 2.9 ± 1.5 , and $0.41 \pm 0.37 \mu\text{g m}^{-3}$, respectively, for the measurement period (Supplemental Fig. S3a). In contrast, the particle number concentrations, N_{420} , are very high compared to other pristine sites (Andreae, 2009), with an average of 3150 (850 – 10300) cm^{-3} , of which a large fraction are in the nucleation mode below 24 nm (average 1100, range 55 – 5250 cm^{-3}) (Fig. 4a).

Deleted: 1

Deleted: 1

Deleted: s.

Deleted: 2

Deleted: extremely

Deleted: .

Formatted: Subscript

Deleted: 2

Deleted: extremely

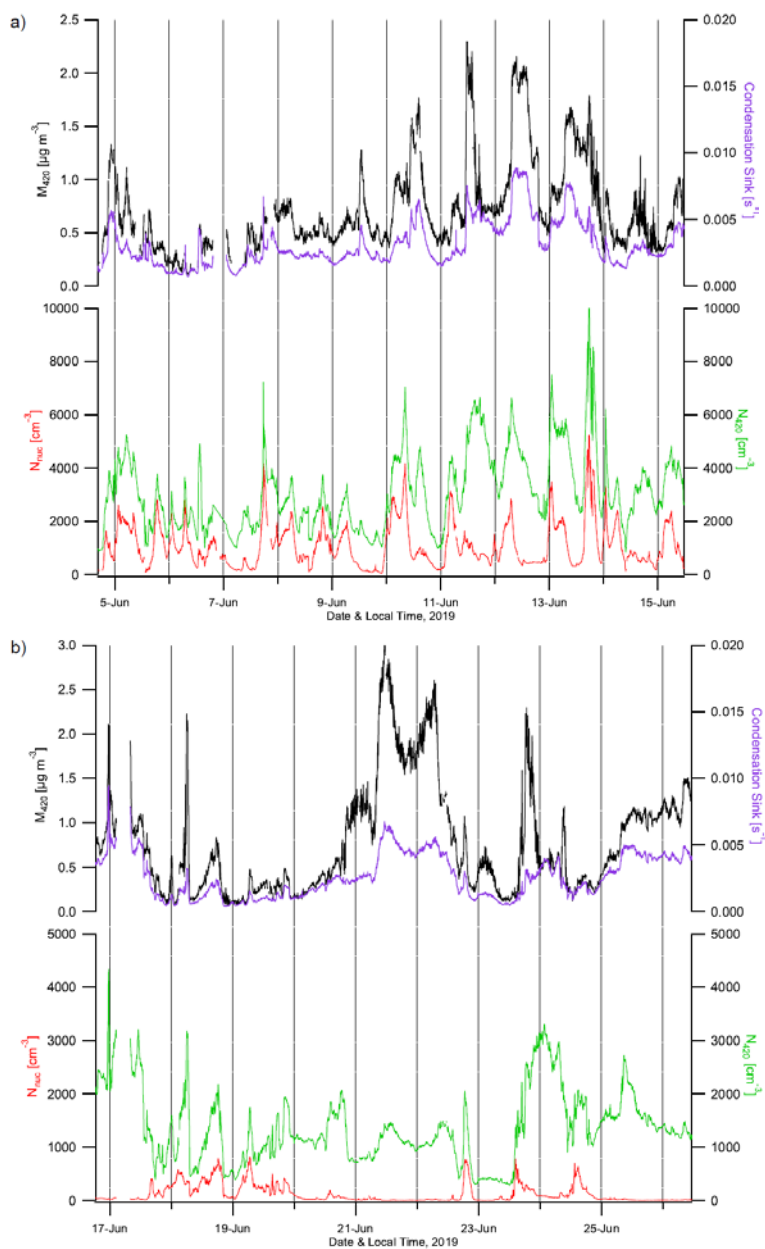


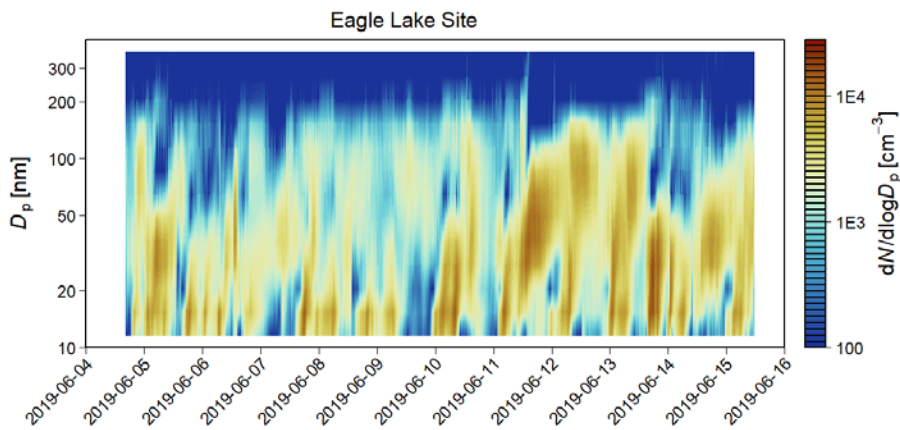
Fig. 4: Mass and number concentrations of aerosol particles <420 nm (M_{420} and N_{420}), number concentrations of nucleation mode particles <24 nm (N_{nuc}), and condensation sink at a) Eagle Lake and b) Nazko River.

325

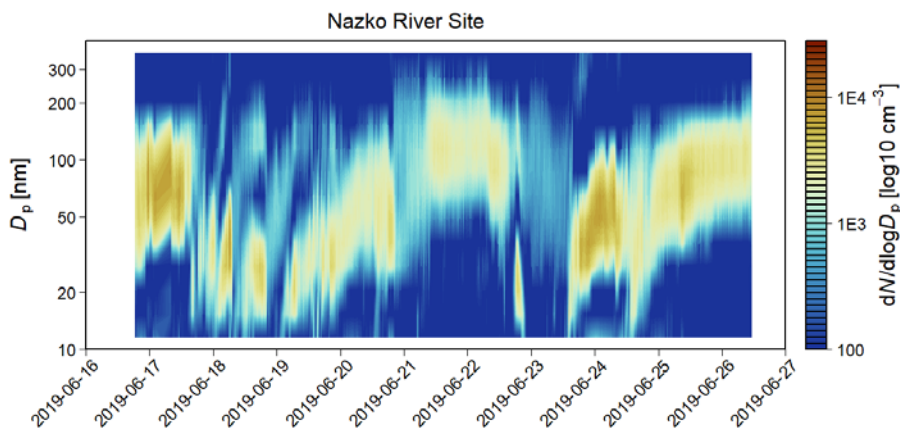
Like at EL, the BC, dust, and seasalt concentrations at the Nazko River site were very low, at 0.063 ± 0.062 , 1.3 ± 0.8 , and $0.34 \pm 0.35 \mu\text{g m}^{-3}$, respectively (Supplemental Fig. S2b). The low BC concentrations indicate the near-absence of combustion-derived pollutants, with the exception of a period during 21-22 Jun, when the backtrajectories indicated transport from the north. During this episode, aerosol mass concentrations, BC, and the accumulation mode number concentrations

330 were slightly elevated (Figs. 4b and 5b), suggesting an influence of smoke from the large fires that were burning since
 mid-May in northern Alberta, about 600-800 km NE of the site. Excluding this period, BC concentrations averaged
 $0.036 \pm 0.017 \mu\text{g m}^{-3}$. The average M_{420} concentrations at NR were similar to those at EL, with an average of 0.77 ± 0.61
 $\mu\text{g m}^{-3}$, which is reduced to $0.57 \pm 0.40 \mu\text{g m}^{-3}$ (range 0.063 – 2.3) when the smoke-affected period is excluded. The number
 concentrations, N_{420} and N_{mic} , were 1350 ± 670 (range 280 – 4340) and 123 ± 165 (range 3 – 820) cm^{-3} , respectively, sub-
 335 stantially lower than at EL.

a)



b)



340 Fig. 5: Time series of aerosol number size distributions at a) Eagle Lake and b) Nazko River.

3.4 New particle formation events

3.4.1 NPF frequency

As discussed in more detail in the Methods section, new particle formation events were identified using the procedure and criteria of Kulmala et al. (2012). The characteristics of the NPF events at our two sites are summarized in Table 1.

Table 1: New particle formation events at the Eagle Lake and Nazko River sites: Timing, condensation sink at the beginning of the event, formation rate at 10 nm, and growth rate.

Event Number	Event Start [Local Time]	Event End [Local Time]	Event Duration [min]	Condensation Sink [s^{-1}]	Formation Rate at 10 nm [$cm^{-3} h^{-1}$]	Growth Rate [$nm h^{-1}$]
Eagle Lake						
1	04-Jun-19 18:40	04-Jun-19 21:00	140	0.0019	0.29	2.0
2	05-Jun-19 00:00	05-Jun-19 05:00	300	0.0046	0.35	1.8
3	05-Jun-19 15:40	05-Jun-19 20:00	260	0.0025	0.26	1.0
4	06-Jun-19 00:00	06-Jun-19 02:30	150	0.0010	0.33	2.4
5	06-Jun-19 06:30	06-Jun-19 10:00	210	0.0012	0.65	2.8
6	06-Jun-19 12:40	06-Jun-19 15:10	150	0.0014	0.40	4.6
7	07-Jun-19 15:30	07-Jun-19 19:35	245	0.0018	0.49	1.6
8	08-Jun-19 00:00	08-Jun-19 07:40	460	0.0027	0.07	0.2
9	08-Jun-19 15:30	08-Jun-19 21:00	330	0.0022	0.15	0.5
10	09-Jun-19 03:10	09-Jun-19 12:50	580	0.0019	0.09	1.0
11	09-Jun-19 22:30	10-Jun-19 04:00	330	0.0020	0.19	1.0
12	10-Jun-19 07:00	10-Jun-19 11:00	240	0.0033	0.47	3.6
13	11-Jun-19 02:00	11-Jun-19 08:30	390	0.0019	0.32	2.1
14	11-Jun-19 09:40	11-Jun-19 21:00	680	0.0026	0.22	2.5
15	12-Jun-19 03:50	12-Jun-19 12:00	490	0.0042	0.16	1.5
16	12-Jun-19 23:30	13-Jun-19 02:00	150	0.0029	0.43	3.5
17	13-Jun-19 05:00	13-Jun-19 08:50	230	0.0048	0.18	1.0
18	13-Jun-19 15:20	13-Jun-19 22:00	400	0.0042	0.59	2.1
19	13-Jun-19 23:30	14-Jun-19 02:00	150	0.0019	0.54	5.2
20	14-Jun-19 04:00	14-Jun-19 09:00	300	0.0016	0.16	1.9
21	15-Jun-19 02:00	15-Jun-19 07:00	300	0.0023	0.34	1.3
	Average		309	0.0025	0.32	2.1
	Standard Deviation		148	0.0011	0.16	1.3
Nazko River						
22	17-Jun-19 15:00	17-Jun-19 20:00	300	0.0030	0.12	2.3
23	18-Jun-19 02:00	18-Jun-19 06:40	280	0.0006	0.07	4.0
24	18-Jun-19 08:00	18-Jun-19 14:30	390	0.0006	0.03	2.4
25	19-Jun-19 02:00	19-Jun-19 12:00	600	0.0006	0.05	1.3
26	23-Jun-19 14:00	23-Jun-19 17:00	180	0.0007	0.33	6.0
27	24-Jun-19 13:40	24-Jun-19 18:00	260	0.0014	0.11	3.3
	Average		335	0.0012	0.12	3.2
	Standard Deviation		146	0.0010	0.11	1.6

Deleted: N

Deleted: The criteria for an NPF event were: (1) a distinct increase of N_{nuc} concentrations, (2) formation of a new nucleation mode persisting for more than two hours, and (3) growth of the nucleation mode over several hours. The NPF event identification was first performed by an automated routine (Franco et al., 2021) and then verified visually on the basis of the daily surface plots of the time series of the number size distributions and the time evolution of N_{nuc} particles. A few events erroneously flagged as NPF by the automated algorithm were removed.

Deleted: ¶

At Eagle Lake, we identified 21 distinct NPF events in a time span of only 12 days, with up to three events within a 24-h period (Table 1 and Fig. 5a). Using the classification of Kulmala et al. (2012), which focuses on event days rather than

single NPF events, all 12 days were event days. We further classified the events into daytime and nighttime events using an adjusted event start time. Since the lower cutoff our instrument is 10 nm, it will detect an event some 3 hours later than an instrument with a cutoff at 3 nm would, given our average GR of 2-3 nm h⁻¹. For the purpose of classifying events as daytime or nighttime, we thus adjusted the start time by subtracting 3 hours from the observed start times listed in Table 1, which are based on detection with a lower cutoff at 10 nm. Events were classified as nighttime NPF, if the adjusted start time fell between 21:00 and 04:30 LT, i.e., the time when the SW radiation flux was typically below 20 W m⁻². Using this criterion, we found 11 nighttime events at EL, with nighttime nucleation occurring on 8 of 11 nights, and in some instances with two events in a single night.

The frequency of NPF was much lower at Nazko River (Fig. 5b), with only six events over 10 days, and five days classified as event days. Nighttime NPF also occurred less frequently, with only three events during the study period. During the smoke-affected period of 21-22 Jun, there was no evidence of NPF, and N_{nuc} levels were very low, with an average of 16 cm⁻³. Nucleation activity resumed immediately, however, around 18 LT on 22 Jun, when accumulation mode concentrations had dropped back down to background values.

Given the relatively short duration of our study compared to the long-term studies at some other sites, we can only make limited comparisons regarding NPF frequency at our BC sites. Our study took place during late spring, when NPF events are most frequent at other temperate/boreal sites, e.g., Hyytiälä (Dada et al., 2017) and Vavihill, Sweden (Kristensson et al., 2008). Similarly, at Pallas, a remote site at the northern edge of the boreal forest (68 °N) in Finland, Asmi et al. (2011) found that NPF event frequency peaked in spring, while the highest growth rates occurred in summer. Taking both our sites together, we had 17 event days out of a total of 23 days of observations, for a frequency of 74%, which is significantly higher than the median frequencies of 20-50% reported for the spring/summer seasons at comparable sites by Nieminen et al. (2018). This is largely a consequence of the frequent nighttime NPF at our sites, because without the nighttime events there would be only 11 NPF days, or a frequency of 48%.

3.4.2 Diurnal behavior

New particle formation events occurred at our sites just as often during nighttime as during daytime (13 out of 27 events), in sharp contrast to what has been observed at most other sites. For example, NPF at Hyytiälä typically takes place between sunrise and noon (Dada et al., 2017), and at Egbert, Ontario, and Whistler Mountain, British Columbia, only daytime NPF was observed (Pierce et al., 2012; Pierce et al., 2014).

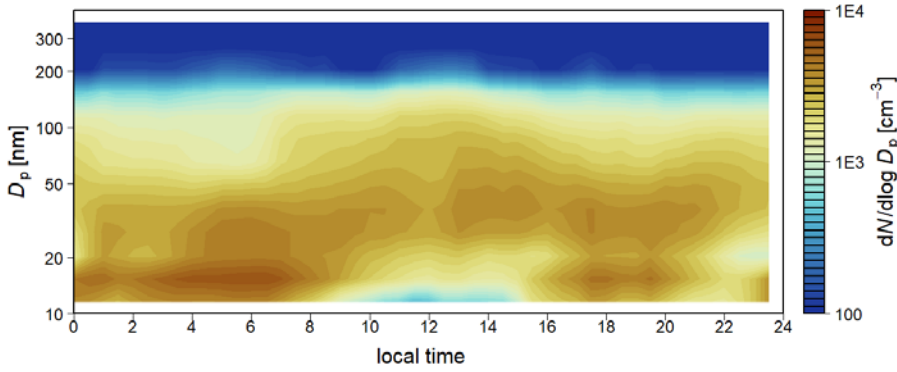
The timing of NPF is further illustrated in Figs. 6 and 7, which show the diurnal variation of the aerosol size spectra averaged over the entire measurement period and for an exemplary day at each site, respectively. At EL, Fig. 6a shows a distinct nucleation mode appearing around 23 LT, representing the nighttime events, which intensifies during the night to reach the highest N_{nuc} concentrations around 06 LT. Growth into the Aitken mode continues throughout the day, and around mid-day the nucleation mode is absent. Another set of NPF events occurs between 16 and 20 LT, also followed by growth into the Aitken mode. At NR (Fig. 6b) we see overall lower total particle concentrations, much lower N_{nuc} concentrations, especially at nighttime, and a relatively more prominent Aitken mode at around 70 nm. The diurnal timing of NPF events is less distinct at NR than at EL, but there is a suggestion of elevated N_{nuc} between 00 and 07 LT, and around 14 LT.

Deleted: 2

Deleted: 7

Deleted: 50

400 a)



b)

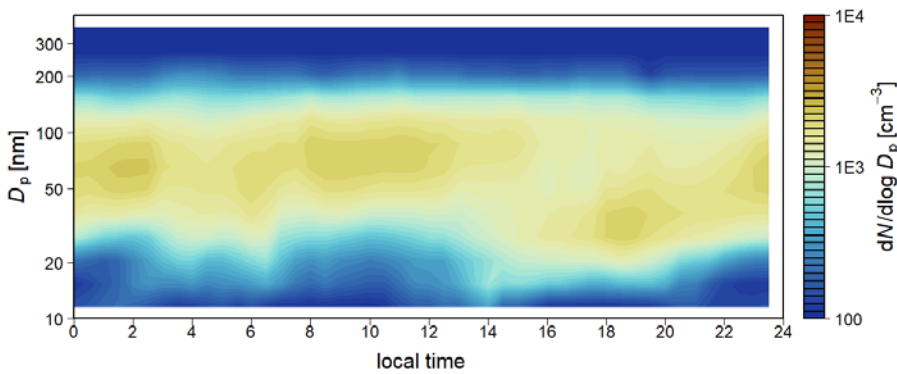


Fig. 6: Diurnal plot of the mean number size distribution of aerosol particles at a) Eagle Lake and b) Nazko River.

405 The details of the aerosol evolution are illustrated for exemplary days in Fig. 7. At EL (Fig. 7a), 11 Jun was a day with very light winds, which resulted in a nearly stationary airmass. After midnight, particle concentrations were quite low, with a faint nucleation mode below 20 nm, an Aitken mode around 50 nm, and a weak accumulation mode around 100 nm. A distinct new nucleation mode appears at 02 LT, which grows throughout the day to ca. 50 nm. Additional minor NPF events are seen in the afternoon and around 23 LT. In contrast, at NR, Fig. 7b shows the near-complete absence of nucleation mode particles on this night, followed by a daytime NPF event with fairly rapid growth into the Aitken range.

Deleted: at

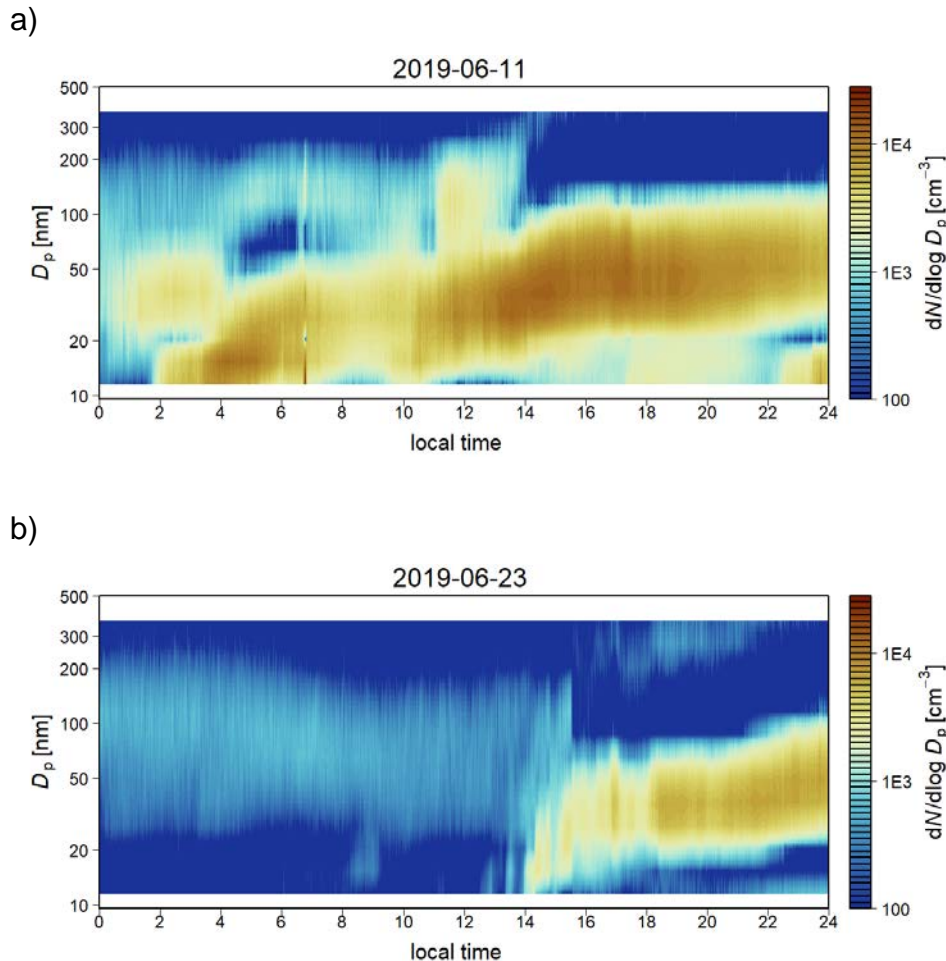


Fig. 7: Time series plots of the aerosol number size distribution of aerosol particles on exemplary days at a) Eagle Lake and b) Nazko River.

3.4.3 Airmass origin

420 As already discussed above in sections 3.2 and 3.3, most of the airmasses sampled at our sites had crossed the Pacific coast 1 – 2 days before arriving at our sites, and contained little or no detectable anthropogenic pollution. Thus, similar to other temperate/boreal sites, e.g., Hyttälä and Pallas, our NPF events occurred in clean airmasses, mostly originating from the west and northwest, which had low levels of pollution aerosols that would suppress nucleation by acting as condensation sink (CS) (Sogacheva et al., 2005; Dada et al., 2017).

425 There was, however, no evidence that a marine influence on the air mass enabled or facilitated NPF at the EL site. The airmasses arriving on 8-13 Jun had not had contact with the sea surface, as they had either remained for the last 48 hours in the continental boundary layer (8 Jun) or had descended from the free troposphere. In these airmasses, NPF was just as active as in the airmasses arriving on 4-7 and 14-15 Jun, which had come from the surface level over the Pacific and had traveled in the boundary layer for their entire 48-h history.

430 On the other hand, even quite small levels of pollution were enough to suppress NPF. The airmasses that had arrived on
21-22 Jun from a region polluted with wildfire smoke had M_{420} concentrations of only $1.5 - 3.0 \mu\text{g m}^{-3}$ and N_{420} concen-
435 trations of ca. $1000 - 1500 \text{ cm}^{-3}$ (Fig. 4b), yet even this small amount of pollution was able to completely suppress NPF.

3.4.4 Condensation sink

The surfaces of preexisting aerosol particles act as a sink for condensable species, such as gaseous H_2SO_4 or extremely-
435 low-volatility organic compounds (ELVOCs), thereby potentially suppressing their concentrations below those required
for nucleation and NPF. The CS at the start of NPF events ranged from 0.0006 to 0.0048 s^{-1} (Table 1), with average values
of $0.0025 \pm 0.0011 \text{ s}^{-1}$ at EL and $0.0012 \pm 0.0010 \text{ s}^{-1}$ at NR. These CS values are similar to those for the NPF event days at
Hyytiälä, which typically fell into the range of 0.002 to 0.004 s^{-1} during June (Dada et al., 2017). At Pallas, event days in
440 spring happened typically at CS in a similar range, between 0.0004 and 0.003 s^{-1} (Asmi et al., 2011). With only one
exception (event 18), all daytime NPF events occurred when CS was below the temperature-dependent threshold value
obtained at Hyytiälä by Dada et al. (2017).

3.4.5 Growth rates

The overall range of GR during our campaign was $0.18 - 6.0 \text{ nm h}^{-1}$, with averages of 2.1 ± 1.2 and $3.4 \pm 1.6 \text{ nm h}^{-1}$ at EL
and NR, respectively. The faster growth at NR may be related to the lower number concentrations at this site. These GR
445 values are in good agreement with median GRs for the spring/summer seasons at the temperate/boreal sites in Eurasia
(Varriö, Pallas, Abisko, Tiksi, Hyytiälä, and Aspöreten), which range between 1.6 and 4.6 nm h^{-1} (Nieminen et al., 2018),
at Egbert, Ontario, where the mean GR was 3.1 nm h^{-1} (Pierce et al., 2014), and at Whistler Mountain, BC, where GRs
were $2-5 \text{ nm h}^{-1}$ (Pierce et al., 2012).

3.4.6 Formation rates

450 ~~Given the lower cutoff of our instrument at 10 nm , we calculated the formation rate of particles $>10 \text{ nm}$, J_{10} , from the rate
of increase of particle number concentrations in the size range $10 - 24 \text{ nm}$ during the early part of the NPF events.~~ At EL,
the average value of J_{10} was $0.32 \pm 0.16 \text{ cm}^{-3} \text{ s}^{-1}$, while at NR the formation rate was much lower, with an average of
 $0.12 \pm 0.11 \text{ cm}^{-3} \text{ s}^{-1}$. Overall, the range of formation rates observed at our sites is in good agreement with the median values
of 0.1 to $0.52 \text{ cm}^{-3} \text{ s}^{-1}$ for the spring/summer seasons at the Scandinavian and Siberian temperate/boreal sites listed by
455 Nieminen et al. (2018). At Egbert, the mean J_{10} was significantly higher, likely due to the substantial anthropogenic SO_2 ,
and thus elevated H_2SO_4 vapor, concentrations at that site (Pierce et al., 2014).

3.5 New particle formation mechanism

In previous studies, nucleation processes based on H_2SO_4 , iodic acid (HIO_3), or ELVOCs have been described as mech-
anisms leading to NPF in terrestrial and coastal environments. Because of the limited information obtained in our cam-
460 paign, especially the lack of gas phase measurements of precursor and nucleating species, we do not have conclusive
evidence regarding the mechanism of NPF at our sites. In the following paragraphs, we will examine the potential mech-
anisms and discuss which one of them is the most consistent with our observations.

Iodic acid has been identified as a nucleating species at coastal sites (Sipilä et al., 2016) and in laboratory studies (He et
al., 2021), and may play an important role in pristine environments, where H_2SO_4 is at very low concentrations. It is,
465 however, unlikely to play a role at our sites, since HIO_3 is formed rapidly near its precursor sources and would lead to
nucleation close to the coast rather than far inland. Particles nucleated at the coast would have grown over the 1-2 days
traveling to our site and would show up in the Aitken mode rather than in the nucleation mode.

Moved up [1]: We estimated the CS at our sites from size distribution data from the Nanoscan and the dust and seasalt concentrations from the MERRA-2 reanalysis, using the equations in Kulmala et al. (2012). The size distribution of dust and seasalt was represented by a single mode at $3.5 \mu\text{m}$ with a geometric standard deviation of 2.0 (Albani et al., 2014). The CS was completely dominated by the submicron aerosol, with dust and seasalt typically contributing less than 1%. For comparability with other sites, we calculated CS using the diffusion coefficient of H_2SO_4 , although, as will be discussed below, it is more likely that the actual condensing species were organic compounds.¶

Deleted: We calculated the growth rates (GR) of the newly formed particles based on the method of Kulmala et al. (2012) by fitting modes to the observed size distributions and deriving the time rate of change of the modal diameter during the growth phase of the NPF event.

Deleted: Given the lower cutoff of our instrument at 10 nm , we were not able to derive an estimate for the actual nucleation rate, J^* . Instead, we calculated the formation rate of particles $>10 \text{ nm}$, J_{10} , from the rate of increase of particle number concentrations in the size range $10 - 24 \text{ nm}$ during the early part of the NPF events, following the method of Kulmala et al. (2012). We applied the correction for the coagulation sink, using the parameterization given in eq. (7) of that paper to derive the coagulation sink from the condensation sink.

495 Nucleation based on H₂SO₄ together with stabilizing species, such as ammonia, water, amines, or organics, is the most
common mechanism identified at sites around the world. This mechanism, however, is active at remote and rural sites
only during daytime, when sufficient H₂SO₄ vapor concentrations can be photochemically produced. At Hyytiälä, for
example, NPF with growth into the nucleation mode occurs only during daytime (Dada et al., 2017). While nighttime
nucleation events are quite common there, the new particles never grow beyond a few nanometers (Junninen et al., 2008).
500 In contrast, at our sites we found that there is no clear preference for daytime NPF, and that nighttime events are about as
frequent as daytime ones. Frequent nighttime NPF would not be expected if marine sulfur emissions, acting as precursors
of H₂SO₄, played an important role at our sites, as proposed by Lawler et al. (2018), who observed that NPF events at
Hyytiälä occurred preferentially in airmasses that had recently been over the ocean. While most of our airmasses had also
had contact with the ocean within the last few days, NPF was just as abundant at night as during daytime, and NPF
505 occurred also in airmasses that had no recent contact with the ocean.

Our observations thus argue strongly for pure organic nucleation based on ELVOC species formed from monoterpenes
by autoxidation and reaction with ozone. The important role of non-photochemical processes is further supported by the
lack of a clear preference of NPF events on clear-sky days, in contrast to what has been observed at Hyytiälä (Dada et al.,
2017). Nighttime nucleation has been observed previously at a limited number of other sites, particularly at clean sites
510 with high emissions of monoterpene precursors. For example, at Tumbarumba, in an Australian eucalypt forest, nighttime
NPF events were 2.5 times as frequent as daytime events during summer/autumn (Lee et al., 2008; Suni et al., 2008). On
the other hand, at Abisko, Sweden, Svenningsson et al. (2008) observed only occasional nighttime events, and at Värriö,
Finland, nighttime NPF only accounted for a small fraction (16 of 147) of events (Vehkamäki et al., 2004). Interestingly,
even though NPF is quite uncommon at the Siberian ZOTTO site, there is also a significant fraction of nighttime NPF
515 among these rare events (Uusitalo et al., 2021).

The ELVOC species supporting nucleation at our sites are most likely HOMs produced from monoterpenes by ozonolysis
and/or autoxidation of peroxy radicals following initial attack by OH (Ehn et al., 2010; Ortega et al., 2012; Bianchi et al.,
2019). The high density of conifers around our sites, especially at EL, is a prolific source of monoterpenes, to the point
that their characteristic odor was perceptible on warm days, especially on 11 and 12 Jun when warm temperatures coin-
520 cided with low wind speeds. These days also produced very strong and sustained NPF events (Fig. 5a).

While the relatively short observation period does not allow a detailed analysis of the relationship between NPF and
ambient temperatures, our data do suggest greater production of N_{nuc} at warmer temperatures. The mean N_{nuc} in the cooler
period from 4 to 10 Jun was 1050±770 cm⁻³ (5-min averaged data, N=1759), whereas during the warmer period from 11
to 15 Jun it was 1180±880 cm⁻³ (N=1283). While this difference is modest, it is significant at p<0.0001. The increase in
525 N_{nuc} with higher temperatures could be caused by increased monoterpene emissions, which favor NPF and particle growth,
as has been shown previously by Kulmala et al. (2004). Temperature effects on the rate of HOM formation and nucleation
are not likely to be important over the limited range of ambient temperatures during our study. Low temperatures decrease
the rate of HOM formation (Frege et al., 2018), but increase nucleation probability due to lower volatility of the oxidation
products, resulting in only a modest net change of the nucleation rates from organic precursors (Simon et al., 2020). While
530 more rapid HOM production during the warmer daytime could lead a build-up of HOMs, followed by NPF at the colder
nighttime temperatures, this effect is likely to be very small for the diurnal temperature range (about 10 °C) at our sites
(Simon et al., 2020).

Other than the diurnal change of relative humidity, there were no systematic RH variations that would allow examination
of the effect of RH on NPF events. Based on previous studies, no strong effects would be expected, anyway. Low RH has
535 been shown to favor NPF (Hamed et al., 2011; Dada et al., 2017). However, the mechanism proposed by Hamed et al.
(2011) is based on reduced H₂SO₄ production due to lower OH at very high humidities (>80 %), which were almost never

present during our study. Reduced H₂SO₄ production would also not affect our proposed NPF mechanism, which is based on pure organic nucleation. The increase of the CS due to hygroscopic growth is also not likely to be significant, since the particles at our BC sites are presumed to be mostly organic and thus are not expected to show strong hygroscopic growth over the range of RH prevailing at our sites. Laboratory studies by Bonn et al. (2002) suggested that water vapor suppresses the formation of ELVOCs from monoterpenes. Note that this effect is a function of absolute, not relative humidity. Contrary to what would be expected from the findings of Bonn et al. (2002), we actually observed higher N_{nuc} during the (warmer) period with higher water vapor mixing ratio (11 – 15 Jun, 6.7±0.9 g kg⁻¹) than during the (cooler) period with lower water vapor (4 – 10 Jun, 4.4±0.8 g kg⁻¹).

Ozone plays a critical role as a key oxidant leading to formation of ELVOCs from monoterpenes (Ehn et al., 2014). The minimum O₃ levels required to initiate NPF with monoterpenes in chamber studies were 10-19 ppb (Ortega et al., 2012). While we have no on-site ozone measurements, the ozone data from nearby sites indicate that there were sufficient O₃ concentrations to fulfill this requirement. The O₃ data from the Williams Lake monitoring site (the closest site to EL) ranged between an average morning low of 13 ppb and a late afternoon high of 34 ppb (<https://envistaweb.env.gov.bc.ca/>, last accessed 20 Jul 2021) for our study period (Supplemental Fig. S4). Hourly data were not available from Quesnel, the closest monitoring site to NR, but data for the daily maximum concentrations showed values similar to Williams Lake. Overall, then, our results are most consistent with a mechanism where HOMs/ELVOCs are formed by ozonolysis and/or OH-initiated autoxidation of monoterpenes followed by pure organic nucleation. The high incidence of nighttime NPF is consistent with the findings of Sulo et al. (2021), who showed that HOM dimers have their maxima during the night, whereas the HOM monomers and H₂SO₄ exhibit daytime maxima. The highest concentrations of both monoterpenes and O₃ can be expected in the late afternoon, which may explain why we frequently observed the onset of events with particles >10 nm around midnight, which, given growth rates of 2-3 nm h⁻¹, would imply that the actual nucleation event began around sunset. Analogously, the nighttime nucleation events at Hyytiälä, typically occur around sunset and are driven by HOMs from monoterpene oxidation (Rose et al., 2018), but in contrast to our sites, at Hyytiälä the particles from nighttime NPF never grow beyond a few nanometers (Junninen et al., 2008). Our observed growth rates, averaging 2.1 and 3.2 nm h⁻¹ for the two sites, are in good agreement with the median GRs attributable to monoterpene oxidation products (1.0 – 3.5 nm h⁻¹) measured at Pallas by Asmi et al. (2011).

The pronounced difference in NPF frequency between our two sites may be related to the difference in vegetation in the two areas. Whereas the landscape around EL is completely dominated by conifers, a large fraction of the area around NR has been deforested in recent years either by logging or wildfires (see Figs. 1b and 1c). These cleared areas are covered by a mixture of herbaceous vegetation, small conifers, and abundant aspens. Consequently, one would expect lower concentrations of monoterpenes coupled with high levels of isoprene emitted by the aspens. Suppression of NPF in an isoprene-dominated forest environment has been observed by Kanawade et al. (2011) and investigated in the laboratory by Kiendler-Scharr et al. (2009), who attributed it to OH scavenging by isoprene. This mechanism is not likely to be important at our sites, since it would only affect daytime nucleation, whereas at NR, nighttime nucleation is also less frequent than at EL. More likely is the alternative mechanism proposed by Heinritzi et al. (2020), wherein isoprene reduces the yield of dimer HOMs with 19 or 20 C atoms (C₂₀), while increasing the yield of the more volatile dimers with 14 or 15 C atoms (C₁₅), thereby reducing the rate of new particle formation.

4 Summary and conclusions

We conducted a pilot study on NPF at two pristine sites in the temperate/boreal transition zone of British Columbia, Canada, extending over 23 days of measurements in June 2019. While the limited duration of our study does place limits on the generalization of our results, the fact that the meteorological conditions during our study were typical of long-term

Deleted: 3

Deleted: We observed a high frequency of NPF events during four weeks of measurements in June 2019

[average conditions at this time of year and that the land cover surrounding our sites was typical of the region does support that our results were not subject to bias from unusual weather or vegetation cover.](#)

[At both sites, we observed a high frequency of NPF events.](#) At the Eagle Lake site, every day was an event day, and many days had multiple NPF events. At Nazko River, the NPF frequency was lower, yet still, 50% of days were event days. In contrast to most sites studied previously, NPF occurred as frequently during nighttime as in daytime, with 14 out of a total of 27 events taking place at night.

Airmass trajectory analysis showed that most of the sampled airmasses had arrived from the Pacific Ocean and traveled over land for 1 – 2 days before arriving at our sites. The terrestrial fetch area has an extremely low population density and no industrial activity, resulting in essentially pristine atmospheric conditions. While a marine contribution to NPF cannot be excluded at our sites due to the limited instrumentation available for our campaign, it is likely not of significance, given that there was no preference for daytime nucleation (as would be expected for HIO₃ or H₂SO₄ as nucleating species) and that NPF events were seen just as frequently on days with no previous ocean contact.

The average condensation sink at the start of events was 0.0025 ± 0.0011 at EL and 0.0012 ± 0.0010 s⁻¹ at NR, well within the range where NPF has been observed at other temperate/boreal sites (Asmi et al., 2011; Dada et al., 2017; Kerminen et al., 2018). The particle growth rates, with averages of 2.1 ± 1.3 and 3.2 ± 1.6 nm h⁻¹ at EL and NR, respectively, were also within the range typically observed during spring/summer at temperate/boreal sites in Eurasia and North America (Kerminen et al., 2018; Nieminen et al., 2018). Because of the relatively high lower cutoff diameter of our instrumentation (10 nm), we could not obtain the actual nucleation rate, J*. The formation rates for particles at 10 nm, J₁₀, averaged 0.32 ± 0.16 and 0.12 ± 0.11 cm⁻³ s⁻¹ at EL and NR, respectively, also comparable to the Scandinavian and Siberian temperate/boreal sites listed by Nieminen et al. (2018).

~~Although the limited data available from our campaign does not allow us to draw firm conclusions about the nucleating species responsible for NPF at our sites, several lines of evidence point to pure organic nucleation as the dominant mechanism. The strongest argument comes from the fact that nighttime NPF was as frequent as daytime NPF, analogous to other sites where organic nucleation has been shown to dominate, and ruling out photochemical production of H₂SO₄ as source of nucleating species at least during the night. The lack of anthropogenic sources of SO₂ and the independence of NPF from marine influence on the sampled airmasses also argues against nucleation driven by H₂SO₄. Finally, the presence of abundant monoterpene sources in the fetch (to the point that they sometimes could be detected by their odor) and the potential dependence of the NPF frequency on the presence of isoprene-emitting vegetation also support organic nucleation as the dominant mechanism.~~

Our results are consistent with the model-derived importance of pure organic NPF in remote regions (Gordon et al., 2017; Zhu and Penner, 2019), however, they raise important questions about the extent to which pristine NPF conditions still exist in the present-day atmosphere. At the vast majority of remote sites studied so far, NPF is exclusively a daytime phenomenon, suggesting dominance of H₂SO₄ as the controlling species. Would these sites have been dominated by pure organic nucleation in pre-industrial times, with frequent nighttime NPF? And, why is NPF so infrequent at the remote subboreal ZOTTO site in central Siberia, which is surrounded by vast coniferous forest (Wiedensohler et al., 2019; Uusitalo et al., 2021)? Possibly, the large distance to anthropogenic sources of SO₂ has allowed it to be fully converted to sulfate aerosol, removing the source of H₂SO₄ while providing a condensation sink that prevents organic nucleation. Is there a sequence of regimes, where at truly pristine conditions, pure organic nucleation dominates, followed by H₂SO₄-driven nucleation with organic-dominated growth in the presence of small amounts of anthropogenic SO₂, again followed by a “nucleation valley of death” where the CS from pollution aerosols suppresses nucleation, and finally the highly polluted regime where there is so much SO₂ that H₂SO₄-driven nucleation can overcome the suppression by the elevated CS?

Formatted: Font: 10 pt

Deleted: White

Our study shows that there is a need for in-depth investigations at pristine continental sites to address these questions. A full set of instrumentation to identify nucleating species and precursors is required to elucidate nucleation and growth mechanisms. Also, our measurements were limited to a relatively short period in late spring to early summer, when previous studies at other sites have shown that both NPF events and HOM dimer precursor concentrations have their seasonal maxima (Nieminen et al., 2018; Sulo et al., 2021). Future studies should include the development of a site for continuous long-term observations to investigate the seasonal and interannual variability of NPF over the remote North American forest regions.

Author contributions

MOA designed the experiments and MOA and TWA carried them out. MOA and FD performed the data analysis and CP provided the land cover and footprint analysis. MOA prepared the manuscript with contributions from all co-authors.

Competing interests

The authors declare that they have no known competing interests that could have influenced the work reported in this paper.

Deleted: .

Acknowledgments

We thank the hosts at our sites, Clay and Marilyn Hett at Eagle Lake, and Curtis and Theresa Sharp at Nazko River, for their hospitality and support. Some analyses and visualizations used in this paper were produced with the Giovanni online data system, developed and maintained by the NASA GES DISC. We thank Zengxin Pan for help with downloading the MERRA-2 data. This research was funded by the Distinguished Scientist Fellowship Program of King Saud University and the Max Planck Society.

Data Availability

The Nanoscan SMPS data is archived on the Edmond data base at <https://dx.doi.org/10.17617/3.7w>. The Modern-Era Retrospective analysis for Research and Applications, version 2 (MERRA-2) data used is available at <https://disc.gsfc.nasa.gov/datasets?project=MERRA-2>.

References

- Albani, S., Mahowald, N. M., Perry, A. T., Scanza, R. A., Zender, C. S., Heavens, N. G., Maggi, V., Kok, J. F., and Otto-Bliesner, B. L., Improved dust representation in the Community Atmosphere Model: Journal of Advances in Modeling Earth Systems, 6, 541-570, doi:10.1002/2013ms000279, 2014.
- Andreae, M. O., Aerosols before pollution: Science, 315, 50-51, 2007.
- Andreae, M. O., Correlation between cloud condensation nuclei concentration and aerosol optical thickness in remote and polluted regions: Atmos. Chem. Phys., 9, 543-556, 2009.
- Andreae, M. O., Acevedo, O. C., Araújo, A., Artaxo, P., Barbosa, C. G. G., Barbosa, H. M. J., Brito, J., Carbone, S., Chi, X., Cintra, B. B. L., da Silva, N. F., Dias, N. L., Dias-Júnior, C. Q., Ditas, F., Ditz, R., Godoi, A. F. L., Godoi, R. H. M., Heimann, M., Hoffmann, T., Kesselmeier, J., Könemann, T., Krüger, M. L., Lavric, J. V., Manzi, A. O., Lopes, A. P., Martins, D. L., Mikhailov, E. F., Moran-Zuloaga, D., Nelson, B. W., Nölscher, A. C., Santos Nogueira, D., Piedade, M. T. F., Pöhlker, C., Pöschl, U., Quesada, C. A., Rizzo, L. V., Ro, C. U.,

- Ruckteschler, N., Sá, L. D. A., de Oliveira Sá, M., Sales, C. B., dos Santos, R. M. N., Saturno, J., Schöngart, J., Sörgel, M., de Souza, C. M., de Souza, R. A. F., Su, H., Targhetta, N., Tóta, J., Trebs, I., Trumbore, S., van Eijck, A., Walter, D., Wang, Z., Weber, B., Williams, J., Winderlich, J., Wittmann, F., Wolff, S., and Yáñez-Serrano, A. M., The Amazon Tall Tower Observatory (ATTO): overview of pilot measurements on ecosystem ecology, meteorology, trace gases, and aerosols: *Atmos. Chem. Phys.*, 15, 10723-10776, doi:10.5194/acp-15-10723-2015, 2015.
- 665 Asmi, E., Kivekas, N., Kerminen, V. M., Komppula, M., Hyvarinen, A. P., Hatakka, J., Viisanen, Y., and Lihavainen, H., Secondary new particle formation in Northern Finland Pallas site between the years 2000 and 2010: *Atmos. Chem. Phys.*, 11, 12959-12972, doi:10.5194/acp-11-12959-2011, 2011.
- 670 Bellouin, N., Quaas, J., Gryspeerdt, E., Kinne, S., Stier, P., Watson-Parris, D., Boucher, O., Carslaw, K. S., Christensen, M., Daniau, A. L., Dufresne, J. L., Feingold, G., Fiedler, S., Forster, P., Gettelman, A., Haywood, J. M., Lohmann, U., Malavelle, F., Mauritsen, T., McCoy, D. T., Myhre, G., Mühlenthal, J., Neubauer, D., Possner, A., Rugenstein, M., Sato, Y., Schulz, M., Schwartz, S. E., Sourdeval, O., Storelvmo, T., Toll, V., Winker, D., and Stevens, B., Bounding global aerosol radiative forcing of climate change: *Rev. Geophys.*, 58, e2019RG000660, doi:10.1029/2019RG000660, 2020.
- 675 Bianchi, F., Kurten, T., Riva, M., Mohr, C., Rissanen, M. P., Roldin, P., Berndt, T., Crouse, J. D., Wennberg, P. O., Mentel, T. F., Wildt, J., Junninen, H., Jokinen, T., Kulmala, M., Worsnop, D. R., Thornton, J. A., Donahue, N., Kjaergaard, H. G., and Ehn, M., Highly Oxygenated Organic Molecules (HOM) from gas-phase autoxidation involving peroxy radicals: A key contributor to atmospheric aerosol: *Chem. Rev.*, 119, 3472-3509, doi:10.1021/acs.chemrev.8b00395, 2019.
- 680 Bianchi, F., Junninen, H., Bigi, A., Sinclair, V. A., Dada, L., Hoyle, C. R., Zha, Q., Yao, L., Ahonen, L. R., Bonasoni, P., Buenrostro Mazon, S., Hutterli, M., Laj, P., Lehtipalo, K., Kangasluoma, J., Kerminen, V. M., Kontkanen, J., Marinoni, A., Mirme, S., Molteni, U., Petäjä, T., Riva, M., Rose, C., Sellegri, K., Yan, C., Worsnop, D. R., Kulmala, M., Baltensperger, U., and Dommen, J., Biogenic particles formed in the Himalaya as an important source of free tropospheric aerosols: *Nature Geoscience*, 14, 4-9, doi:10.1038/s41561-020-00661-5, 2021.
- 685 Bonn, B., Schuster, G., and Moortgat, G. K., Influence of water vapor on the process of new particle formation during monoterpene ozonolysis: *J. Phys. Chem. A*, 106, 2869-2881, doi:10.1021/jp012713p, 2002.
- 690 Boucher, O., Randall, D., Artaxo, P., Bretherton, C., Feingold, G., Forster, P., Kerminen, V.-M., Kondo, Y., Liao, H., Lohmann, U., Rasch, P., Satheesh, S. K., Sherwood, S., Stevens, B., and Zhang, X. Y., Clouds and Aerosols, in *Climate Change 2013: The Physical Science Basis*, edited by T. F. Stocker, D. Qin, G.-K. Plattner, M. Tignor, S. K. Allen, J. Boschung, A. Nauels, Y. Xia, V. Bex, & P. M. Midgley, pp. 571-657, Cambridge University Press, Cambridge, UK, and New York, NY, USA, 2013.
- 700 Bousiotis, D., Pope, F. D., Beddows, D. C. S., Dall'Osto, M., Massling, A., Nøjgaard, J. K., Nordstrøm, C., Niemi, J. V., Portin, H., Petäjä, T., Perez, N., Alastuey, A., Querol, X., Kouvarakis, G., Mihalopoulos, N., Vratolis, S., Eleftheriadis, K., Wiedensohler, A., Weinhold, K., Merkel, M., Tuch, T., and Harrison, R. M., A phenomenology of new particle formation (NPF) at 13 European sites: *Atmos. Chem. Phys.*, 21, 11905-11925, doi:10.5194/acp-21-11905-2021, 2021.
- 705 Brean, J., Dall'Osto, M., Simó, R., Shi, Z., Beddows, D. C. S., and Harrison, R. M., Open ocean and coastal new particle formation from sulfuric acid and amines around the Antarctic Peninsula: *Nature Geoscience*, 14, 383-388, doi:10.1038/s41561-021-00751-y, 2021.
- 710 Carslaw, K. S., Lee, L. A., Reddington, C. L., Pringle, K. J., Rap, A., Forster, P. M., Mann, G. W., Spracklen, D. V., Woodhouse, M. T., Regayre, L. A., and Pierce, J. R., Large contribution of natural aerosols to uncertainty in indirect forcing: *Nature*, 503, 67-71, doi:10.1038/nature12674, 2013.
- 715 Carslaw, K. S., Gordon, H., Hamilton, D. S., Johnson, J. S., Regayre, L. A., Yoshioka, M., and Pringle, K. J., Aerosols in the pre-industrial atmosphere: *Current Climate Change Reports*, 3, 1-15, doi:10.1007/s40641-017-0061-2, 2017.
- Dada, L., Paasonen, P., Nieminen, T., Buenrostro Mazon, S., Kontkanen, J., Peräkylä, O., Lehtipalo, K., Hussein, T., Petäjä, T., Kerminen, V. M., Bäck, J., and Kulmala, M., Long-term analysis of clear-sky new particle formation events and nonevents in Hyytiälä: *Atmos. Chem. Phys.*, 17, 6227-6241, doi:10.5194/acp-17-6227-2017, 2017.
- 720 Dada, L., Chellapermal, R., Buenrostro Mazon, S., Paasonen, P., Lampilahti, J., Manninen, H. E., Junninen, H., Petäjä, T., Kerminen, V. M., and Kulmala, M., Refined classification and

- characterization of atmospheric new-particle formation events using air ions: *Atmos. Chem. Phys.*, 18, 17883-17893, doi:10.5194/acp-18-17883-2018, 2018.
- 725 Dal Maso, M., Sogacheva, L., Anisimov, M. P., Arshinov, M., Baklanov, A., Belan, B., Khodzher, T. V., Obolkin, V. A., Staroverova, A., Vlasov, A., Zagaynov, V. A., Lushnikov, A., Lyubovtseva, Y. S., Riipinen, I., Kerminen, V.-M., and Kulmala, M., Aerosol particle formation events at two Siberian stations inside the boreal forest: *Boreal Environment Research*, 13, 81-92, 2008.
- 730 Dal Maso, M., Liao, L., Wildt, J., Kiendler-Scharr, A., Kleist, E., Tillmann, R., Sipilä, M., Hakala, J., Lehtipalo, K., Ehn, M., Kerminen, V. M., Kulmala, M., Worsnop, D., and Mentel, T., A chamber study of the influence of boreal BVOC emissions and sulfuric acid on nanoparticle formation rates at ambient concentrations: *Atmos. Chem. Phys.*, 16, 1955-1970, doi:10.5194/acp-16-1955-2016, 2016.
- 735 Dunn, M. J., Jimenez, J. L., Baumgardner, D., Castro, T., McMurry, P. H., and Smith, J. N., Measurements of Mexico City nanoparticle size distributions: Observations of new particle formation and growth: *Geophys. Res. Lett.*, 31, L10102, doi:10.1029/2004GL019483, 2004.
- 740 Dunne, E. M., Gordon, H., Kürten, A., Almeida, J., Duplissy, J., Williamson, C., Ortega, I. K., Pringle, K. J., Adamov, A., Baltensperger, U., Barmet, P., Benduhn, F., Bianchi, F., Breitenlechner, M., Clarke, A., Curtius, J., Dommen, J., Donahue, N. M., Ehrhart, S., Flagan, R. C., Franchin, A., Guida, R., Hakala, J., Hansel, A., Heinritzi, M., Jokinen, T., Kangasluoma, J., Kirkby, J., Kulmala, M., Kupc, A., Lawler, M. J., Lehtipalo, K., Makhmutov, V., Mann, G., Mathot, S., Merikanto, J., Miettinen, P., Nenes, A., Onnela, A., Rap, A., Reddington, C. L. S., Riccobono, F., Richards, N. A. D., Rissanen, M. P., Rondo, L., Sarnela, N., Schobesberger, S., Sengupta, K., Simon, M., Sipilä, M., Smith, J. N., Stozkhov, Y., Tomé, A., Tröstl, J., Wagner, P. E., Wimmer, D., Winkler, P. M., Worsnop, D. R., and Carslaw, K. S., Global atmospheric particle formation from CERN CLOUD measurements: *Science*, 354, 1119-1124, doi:10.1126/science.aaf2649, 2016.
- 745 Ehn, M., Junninen, H., Petaja, T., Kurten, T., Kerminen, V. M., Schobesberger, S., Manninen, H. E., Ortega, I. K., Vehkamäki, H., Kulmala, M., and Worsnop, D. R., Composition and temporal behavior of ambient ions in the boreal forest: *Atmos. Chem. Phys.*, 10, 8513-8530, doi:10.5194/acp-10-8513-2010, 2010.
- 750 Ehn, M., Thornton, J. A., Kleist, E., Sipilä, M., Junninen, H., Pullinen, I., Springer, M., Rubach, F., Tillmann, R., Lee, B., Lopez-Hilfiker, F., Andres, S., Acir, I. H., Rissanen, M., Jokinen, T., Schobesberger, S., Kangasluoma, J., Kontkanen, J., Nieminen, T., Kurten, T., Nielsen, L. B., Jorgensen, S., Kjaergaard, H. G., Canagaratna, M., Dal Maso, M., Berndt, T., Petaja, T., Wahner, A., Kerminen, V. M., Kulmala, M., Worsnop, D. R., Wildt, J., and Mentel, T. F., A large source of low-volatility secondary organic aerosol: *Nature*, 506, 476-479, doi:10.1038/nature13032, 2014.
- 755 Franco, M. A., Ditas, F., Krempel, L. A., Machado, L. A. T., Andreae, M. O., Araújo, A., Barbosa, H. M. J., de Brito, J. F., Carbone, S., Holanda, B. A., Morais, F. G., Nascimento, J. P., Pöhlker, M. L., Rizzo, L. V., Sá, M., Saturno, J., Walter, D., Wolff, S., Pöschl, U., Artaxo, P., and Pöhlker, C., Occurrence and growth of sub-50 nm aerosol particles in the Amazonian boundary layer: *Atmos. Chem. Phys. Discuss.*, 2021, doi:10.5194/acp-2021-765, 2021.
- 760 Frege, C., Ortega, I. K., Rissanen, M. P., Praplan, A. P., Steiner, G., Heinritzi, M., Ahonen, L., Amorim, A., Bernhammer, A. K., Bianchi, F., Brilke, S., Breitenlechner, M., Dada, L., Dias, A., Duplissy, J., Ehrhart, S., El-Haddad, I., Fischer, L., Fuchs, C., Garmash, O., Gonin, M., Hansel, A., Hoyle, C. R., Jokinen, T., Junninen, H., Kirkby, J., Kürten, A., Lehtipalo, K., Leiminger, M., Mauldin, R. L., Molteni, U., Niehman, L., Petäjä, T., Sarnela, N., Schobesberger, S., Simon, M., Sipilä, M., Stolzenburg, D., Tomé, A., Vogel, A. L., Wagner, A. C., Wagner, R., Xiao, M., Yan, C., Ye, P., Curtius, J., Donahue, N. M., Flagan, R. C., Kulmala, M., Worsnop, D. R., Winkler, P. M., Dommen, J., and Baltensperger, U., Influence of temperature on the molecular composition of ions and charged clusters during pure biogenic nucleation: *Atmos. Chem. Phys.*, 18, 65-79, doi:10.5194/acp-18-65-2018, 2018.
- 765 Giamarelou, M., Eleftheriadis, K., Nyeki, S., Tunved, P., Torseth, K., and Biskos, G., Indirect evidence of the composition of nucleation mode atmospheric particles in the high Arctic: *J. Geophys. Res.*, 121, 965-975, doi:10.1002/2015jd023646, 2016.
- 770 Gordon, H., Sengupta, K., Rap, A., Duplissy, J., Frege, C., Williamson, C., Heinritzi, M., Simon, M., Yan, C., Almeida, J., Tröstl, J., Nieminen, T., Ortega, I. K., Wagner, R., Dunne, E. M., Adamov, A., Amorim, A., Bernhammer, A.-K., Bianchi, F., Breitenlechner, M., Brilke, S., Chen, X., Craven, J. S., Dias, A., Ehrhart, S., Fischer, L., Flagan, R. C., Franchin, A., Fuchs, C., Guida, R., Hakala, J., Hoyle, C. R., Jokinen, T., Junninen, H., Kangasluoma, J., Kim, J., Kirkby, J., Krapf, M., Kürten, A., Laaksonen, A., Lehtipalo, K., Makhmutov, V., Mathot, S.,

785 Molteni, U., Monks, S. A., Onnela, A., Peräkylä, O., Piel, F., Petäjä, T., Praplan, A. P.,
 Pringle, K. J., Richards, N. A. D., Rissanen, M. P., Rondo, L., Sarnela, N., Schobesberger, S.,
 Scott, C. E., Seinfeld, J. H., Sharma, S., Sipilä, M., Steiner, G., Stozhkov, Y., Stratmann, F.,
 Tomé, A., Virtanen, A., Vogel, A. L., Wagner, A. C., Wagner, P. E., Weingartner, E.,
 Wimmer, D., Winkler, P. M., Ye, P., Zhang, X., Hansel, A., Dommen, J., Donahue, N. M.,
 790 Worsnop, D. R., Baltensperger, U., Kulmala, M., Curtius, J., and Carslaw, K. S., Reduced
 anthropogenic aerosol radiative forcing caused by biogenic new particle formation: Proc.
 Natl. Acad. Sci., 113, 12,053-12,058, doi:10.1073/pnas.1602360113, 2016.

Gordon, H., Kirkby, J., Baltensperger, U., Bianchi, F., Breitenlechner, M., Curtius, J., Dias, A.,
 Dommen, J., Donahue, N. M., Dunne, E. M., Duplissy, J., Ehrhart, S., Flagan, R. C., Frege,
 C., Fuchs, C., Hansel, A., Hoyle, C. R., Kulmala, M., Kürten, A., Lehtipalo, K., Makhmutov,
 795 V., Molteni, U., Rissanen, M. P., Stozhkov, Y., Tröstl, J., Tsagkogeorgas, G., Wagner, R.,
 Williamson, C., Wimmer, D., Winkler, P. M., Yan, C., and Carslaw, K. S., Causes and
 importance of new particle formation in the present-day and pre-industrial atmospheres: J.
 Geophys. Res., 122, 8739-8760, doi:10.1002/2017JD026844, 2017.

Hamed, A., Korhonen, H., Sihto, S. L., Joutsensaari, J., Jarvinen, H., Petaja, T., Arnold, F., Nieminen,
 800 T., Kulmala, M., Smith, J. N., Lehtinen, K. E. J., and Laaksonen, A., The role of relative
 humidity in continental new particle formation: J. Geophys. Res., 116, D03202,
 doi:10.1029/2010jd014186, 2011.

Hamilton, D. S., Hantson, S., Scott, C. E., Kaplan, J. O., Pringle, K. J., Nieradzik, L. P., Rap, A.,
 Folberth, G. A., Spracklen, D. V., and Carslaw, K. S., Reassessment of pre-industrial fire
 805 emissions strongly affects anthropogenic aerosol forcing: Nature Communications, 9, 3182,
 doi:10.1038/s41467-018-05592-9, 2018.

He, X. C., Tham, Y. J., Dada, L., Wang, M. Y., Finkenzeller, H., Stolzenburg, D., Iyer, S., Simon,
 M., Kurten, A., Shen, J. L., Rorup, B., Rissanen, M., Schobesberger, S., Baalbaki, R., Wang,
 D. S., Koenig, T. K., Jokinen, T., Sarnela, N., Beck, L. J., Almeida, J., Amanatidis, S.,
 810 Amorim, A., Ataei, F., Baccharini, A., Bertozzi, B., Bianchi, F., Brilke, S., Caudillo, L., Chen,
 D. X., Chiu, R., Chu, B. W., Dias, A., Ding, A. J., Dommen, J., Duplissy, J., El Haddad, I.,
 Carracedo, L. G., Granzin, M., Hansel, A., Heinritzi, M., Hofbauer, V., Junninen, H.,
 Kangasluoma, J., Kempainen, D., Kim, C., Kong, W. M., Krechmer, J. E., Kvashin, A.,
 Laitinen, T., Lamkaddam, H., Lee, C. P., Lehtipalo, K., Leiminger, M., Li, Z. J., Makhmutov,
 815 V., Manninen, H. E., Marie, G., Marten, R., Mathot, S., Mauldin, R. L., Mentler, B., Mohler,
 O., Muller, T., Nie, W., Onnela, A., Petaja, T., Pfeifer, J., Philippov, M., Ranjithkumar, A.,
 Saiz-Lopez, A., Salma, I., Scholz, W., Schuchmann, S., Schulze, B., Steiner, G., Stozhkov,
 Y., Tauber, C., Tome, A., Thakur, R. C., Vaisanen, O., Vazquez-Pufleau, M., Wagner, A. C.,
 Wang, Y. H., Weber, S. K., Winkler, P. M., Wu, Y. S., Xiao, M., Yan, C., Ye, Q., Ylisirnio,
 820 A., Zauer-Wieczorek, M., Zha, Q. Z., Zhou, P. T., Flagan, R. C., Curtius, J., Baltensperger,
 U., Kulmala, M., Kerminen, V. M., Kurten, T., Donahue, N. M., Volkamer, R., Kirkby, J.,
 Worsnop, D. R., and Sipilä, M., Role of iodine oxoacids in atmospheric aerosol nucleation:
 Science, 371, 589-595, doi:10.1126/science.abe0298, 2021.

Heinritzi, M., Dada, L., Simon, M., Stolzenburg, D., Wagner, A. C., Fischer, L., Ahonen, L. R.,
 825 Amanatidis, S., Baalbaki, R., Baccharini, A., Bauer, P. S., Baumgartner, B., Bianchi, F., Brilke,
 S., Chen, D., Chiu, R., Dias, A., Dommen, J., Duplissy, J., Finkenzeller, H., Frege, C., Fuchs,
 C., Garmash, O., Gordon, H., Granzin, M., El Haddad, I., He, X., Helm, J., Hofbauer, V.,
 Hoyle, C. R., Kangasluoma, J., Keber, T., Kim, C., Kürten, A., Lamkaddam, H., Laurila, T.
 M., Lampilahti, J., Lee, C. P., Lehtipalo, K., Leiminger, M., Mai, H., Makhmutov, V.,
 830 Manninen, H. E., Marten, R., Mathot, S., Mauldin, R. L., Mentler, B., Molteni, U., Müller,
 T., Nie, W., Nieminen, T., Onnela, A., Partoll, E., Passananti, M., Petäjä, T., Pfeifer, J.,
 Pospisilova, V., Quéléver, L. L. J., Rissanen, M. P., Rose, C., Schobesberger, S., Scholz, W.,
 Scholze, K., Sipilä, M., Steiner, G., Stozhkov, Y., Tauber, C., Tham, Y. J., Vazquez-Pufleau,
 M., Virtanen, A., Vogel, A. L., Volkamer, R., Wagner, R., Wang, M., Weitz, L., Wimmer,
 835 D., Xiao, M., Yan, C., Ye, P., Zha, Q., Zhou, X., Amorim, A., Baltensperger, U., Hansel, A.,
 Kulmala, M., Tomé, A., Winkler, P. M., Worsnop, D. R., Donahue, N. M., Kirkby, J., and
 Curtius, J., Molecular understanding of the suppression of new-particle formation by
 isoprene: Atmos. Chem. Phys., 20, 11809-11821, doi:10.5194/acp-20-11809-2020, 2020.

Huneus, N., Chevallier, F., and Boucher, O., Estimating aerosol emissions by assimilating observed
 840 aerosol optical depth in a global aerosol model: Atmos. Chem. Phys., 12, 4585-4606,
 doi:10.5194/acp-12-4585-2012, 2012.

Jokinen, T., Berndt, T., Makkonen, R., Kerminen, V.-M., Junninen, H., Paasonen, P., Stratmann, F.,
 Herrmann, H., Guenther, A. B., Worsnop, D. R., Kulmala, M., Ehn, M., and Sipilä, M.,
 Production of extremely low volatile organic compounds from biogenic emissions: Measured

845 yields and atmospheric implications: *Proc. Natl. Acad. Sci.*, 112, 7123-7128,
doi:10.1073/pnas.1423977112, 2015.

Junninen, H., Hulkkonen, M., Riipinen, I., Nieminen, T., Hirsikko, A., Suni, T., Boy, M., Lee, S.-H.,
Vana, M., Tammet, H., Kerminen, V.-M., and Kulmala, M., Observations on nocturnal
850 growth of atmospheric clusters: *Tellus B*, 60, 365-371, doi:10.1111/j.1600-
0889.2008.00356.x, 2008.

Kanawade, V. P., Jobson, B. T., Guenther, A. B., Erupe, M. E., Pressley, S. N., Tripathi, S. N., and
Lee, S. H., Isoprene suppression of new particle formation in a mixed deciduous forest:
Atmos. Chem. Phys., 11, 6013-6027, doi:10.5194/acp-11-6013-2011, 2011.

Kerminen, V. M., Chen, X. M., Vakkari, V., Petaja, T., Kulmala, M., and Bianchi, F., Atmospheric
855 new particle formation and growth: review of field observations: *Environmental Research
Letters*, 13, 103003, doi:10.1088/1748-9326/aadf3c, 2018.

Kiendler-Scharr, A., Wildt, J., Dal Maso, M., Hohaus, T., Kleist, E., Mentel, T. F., Tillmann, R.,
Uerlings, R., Schurr, U., and Wahner, A., New particle formation in forests inhibited by
isoprene emissions: *Nature*, 461, 381-384, doi:10.1038/nature08292, 2009.

860 Kirkby, J., Duplissy, J., Sengupta, K., Frege, C., Gordon, H., Williamson, C., Heinritzi, M., Simon,
M., Yan, C., Almeida, J., Tröstl, J., Nieminen, T., Ortega, I. K., Wagner, R., Adamov, A.,
Amorim, A., Bernhammer, A.-K., Bianchi, F., Breitenlechner, M., Brilke, S., Chen, X.,
Craven, J., Dias, A., Ehrhart, S., Flagan, R. C., Franchin, A., Fuchs, C., Guida, R., Hakala, J.,
865 Hoyle, C. R., Jokinen, T., Junninen, H., Kangasluoma, J., Kim, J., Krapf, M., Kürten, A.,
Laaksonen, A., Lehtipalo, K., Makhmutov, V., Mathot, S., Molteni, U., Onnela, A., Peräkylä,
O., Piel, F., Petäjä, T., Praplan, A. P., Pringle, K., Rap, A., Richards, N. A. D., Riipinen, I.,
Rissanen, M. P., Rondo, L., Sarnela, N., Schobesberger, S., Scott, C. E., Seinfeld, J. H., Sipilä,
M., Steiner, G., Stozhkov, Y., Stratmann, F., Tomé, A., Virtanen, A., Vogel, A. L., Wagner,
A. C., Wagner, P. E., Weingartner, E., Wimmer, D., Winkler, P. M., Ye, P., Zhang, X., Hansel,
870 A., Dommen, J., Donahue, N. M., Worsnop, D. R., Baltensperger, U., Kulmala, M., Carslaw,
K. S., and Curtius, J., Ion-induced nucleation of pure biogenic particles: *Nature*, 533, 521-
526, doi:10.1038/nature17953, 2016.

Kontkanen, J., Järvinen, E., Manninen, H. E., Lehtipalo, K., Kangasluoma, J., Decesari, S., Gobbi,
G. P., Laaksonen, A., Petäjä, T., and Kulmala, M., High concentrations of sub-3nm clusters
875 and frequent new particle formation observed in the Po Valley, Italy, during the PEGASOS
2012 campaign: *Atmos. Chem. Phys.*, 16, 1919-1935, doi:10.5194/acp-16-1919-2016, 2016.

Kristensson, A., Dal Maso, M., Swietlicki, E., Hussein, T., Zhou, J., Kerminen, V. M., and Kulmala,
M., Characterization of new particle formation events at a background site in Southern
880 Sweden: relation to air mass history: *Tellus B*, 60, 330-344, doi:10.1111/j.1600-
0889.2008.00345.x, 2008.

Kulmala, M., Vehkamäki, H., Petajda, T., Dal Maso, M., Lauri, A., Kerminen, V. M., Birmili, W.,
and McMurry, P. H., Formation and growth rates of ultrafine atmospheric particles: a review
of observations: *J. Aerosol Sci.*, 35, 143-176, 2004.

Kulmala, M., Petäjä, T., Nieminen, T., Sipilä, M., Manninen, H. E., Lehtipalo, K., Dal Maso, M.,
885 Aalto, P. P., Junninen, H., Paasonen, P., Riipinen, I., Lehtinen, K. E. J., Laaksonen, A., and
Kerminen, V.-M., Measurement of the nucleation of atmospheric aerosol particles: *Nat.
Protocols*, 7, 1651-1667, doi:10.1038/nprot.2012.091, 2012.

Kulmala, M., Kontkanen, J., Junninen, H., Lehtipalo, K., Manninen, H. E., Nieminen, T., Petaja, T.,
Sipila, M., Schobesberger, S., Rantala, P., Franchin, A., Jokinen, T., Jarvinen, E., Aijala, M.,
890 Kangasluoma, J., Hakala, J., Aalto, P. P., Paasonen, P., Mikkilä, J., Vanhanen, J., Aalto, J.,
Hakola, H., Makkonen, U., Ruuskanen, T., Mauldin, R. L., Duplissy, J., Vehkamäki, H., Back,
J., Kortelainen, A., Riipinen, I., Kurten, T., Johnston, M. V., Smith, J. N., Ehn, M., Mentel,
T. F., Lehtinen, K. E. J., Laaksonen, A., Kerminen, V. M., and Worsnop, D. R., Direct
895 observations of atmospheric aerosol nucleation: *Science*, 339, 943-946,
doi:10.1126/science.1227385, 2013.

Kürten, A., Li, C. X., Bianchi, F., Curtius, J., Dias, A., Donahue, N. M., Duplissy, J., Flagan, R. C.,
Hakala, J., Jokinen, T., Kirkby, J., Kulmala, M., Laaksonen, A., Lehtipalo, K., Makhmutov,
V., Onnela, A., Rissanen, M. P., Simon, M., Sipilä, M., Stozhkov, Y., Tröstl, J., Ye, P. L., and
900 McMurry, P. H., New particle formation in the sulfuric acid-dimethylamine-water system:
reevaluation of CLOUD chamber measurements and comparison to an aerosol nucleation and
growth model: *Atmos. Chem. Phys.*, 18, 845-863, doi:10.5194/acp-18-845-2018, 2018.

Kyrö, E. M., Väänänen, R., Kerminen, V. M., Virkkula, A., Petäjä, T., Asmi, A., Dal Maso, M.,
Nieminen, T., Juhola, S., Shcherbinin, A., Riipinen, I., Lehtipalo, K., Keronen, P., Aalto, P.
P., Hari, P., and Kulmala, M., Trends in new particle formation in eastern Lapland, Finland:

905 effect of decreasing sulfur emissions from Kola Peninsula: *Atmos. Chem. Phys.*, 14, 4383-4396, doi:10.5194/acp-14-4383-2014, 2014.

Lawler, M. J., Rissanen, M. P., Ehn, M., Mauldin, R. L., Sarnela, N., Sipila, M., and Smith, J. N., Evidence for diverse biogeochemical drivers of boreal forest new particle formation: *Geophys. Res. Lett.*, 45, 2038-2046, doi:10.1002/2017gl076394, 2018.

910 Lee, S.-H., Young, L.-H., Benson, D. R., Suni, T., Kulmala, M., Junninen, H., Campos, T. L., Rogers, D. C., and Jensen, J., Observations of nighttime new particle formation in the troposphere: *J. Geophys. Res.*, 113, D10210, doi:10.1029/2007jd009351, 2008.

Lehtipalo, K., Yan, C., Dada, L., Bianchi, F., Xiao, M., Wagner, R., Stolzenburg, D., Ahonen, L. R., Amorim, A., Baccarini, A., Bauer, P. S., Baumgartner, B., Bergen, A., Bernhammer, A.-K., Breitenlechner, M., Brilke, S., Buchholz, A., Mazon, S. B., Chen, D., Chen, X., Dias, A., Dommen, J., Draper, D. C., Duplissy, J., Ehn, M., Finkenzeller, H., Fischer, L., Frege, C., Fuchs, C., Garmash, O., Gordon, H., Hakala, J., He, X., Heikkinen, L., Heinritzi, M., Helm, J. C., Hofbauer, V., Hoyle, C. R., Jokinen, T., Kangasluoma, J., Kerminen, V.-M., Kim, C., Kirkby, J., Kontkanen, J., Kuerten, A., Lawler, M. J., Mai, H., Mathot, S., Mauldin, R. L., III, Molteni, U., Nichman, L., Nie, W., Nieminen, T., Ojdanic, A., Onnela, A., Passananti, M., Petaja, T., Piel, F., Pospisilova, V., Quelever, L. L. J., Rissanen, M. P., Rose, C., Sarnela, N., Schallhart, S., Schuchmann, S., Sengupta, K., Simon, M., Sipila, M., Tauber, C., Tome, A., Trostl, J., Vaisanen, O., Vogel, A. L., Volkamer, R., Wagner, A. C., Wang, M., Weitz, L., Wimmer, D., Ye, P., Ylisirnio, A., Zha, Q., Carslaw, K. S., Curtius, J., Donahue, N. M., Flagan, R. C., Hansel, A., Riipinen, I., Virtanen, A., Winkler, P. M., Baltensperger, U., Kulmala, M., and Worsnop, D. R., Multicomponent new particle formation from sulfuric acid, ammonia, and biogenic vapors: *Science Advances*, 4, eaau5363, doi:10.1126/sciadv.aau5363, 2018.

925 Merikanto, J., Spracklen, D. V., Mann, G. W., Pickering, S. J., and Carslaw, K. S., Impact of nucleation on global CCN: *Atmos. Chem. Phys.*, 9, 8601-8616, 2009.

930 Mortier, A., Gliss, J., Schulz, M., Aas, W., Andrews, E., Bian, H., Chin, M., Ginoux, P., Hand, J., Holben, B., Hua, Z., Kipling, Z., Kirkevåg, A., Laj, P., Lurton, T., Myhre, G., Neubauer, D., Olivie, D., von Salzen, K., Takemura, T., and Tilmes, S., Evaluation of climate model aerosol trends with ground-based observations over the last two decades - an AeroCom and CMIP6 analysis: *Atmos. Chem. Phys. Discuss.*, 2020, 1-36, doi:10.5194/acp-2019-1203, 2020.

935 Naik, V., Szopa, S., Adhikary, B., Artaxo, P., Berntsen, T., Collins, W. D., Fuzzi, S., Gallardo, L., Kiendler-Scharr, A., Klimont, Z., Liao, H., Unger, N., and Zanis, P., Short-Lived Climate Forcers, in *Climate Change 2021: The Physical Science Basis. Contribution of Working Group I to the Sixth Assessment Report of the Intergovernmental Panel on Climate Change*, edited by V. Masson-Delmotte, P. Zhai, A. Pirani, S. L. Connors, C. Péan, S. Berger, N. Caud, Y. Chen, L. Goldfarb, M. I. Gomis, M. Huang, K. Leitzell, E. Lonnoy, J. B. R. Matthews, T. K. Maycock, T. Waterfield, O. Yelekçi, R. Yu, & B. Zhou, pp. In Press, Cambridge University Press, 2021.

940 Nieminen, T., Kerminen, V. M., Petäjä, T., Aalto, P. P., Arshinov, M., Asmi, E., Baltensperger, U., Beddows, D. C. S., Beukes, J. P., Collins, D., Ding, A., Harrison, R. M., Henzing, B., Hooda, R., Hu, M., Hörrak, U., Kivekäs, N., Komsaare, K., Krejci, R., Kristensson, A., Laakso, L., Laaksonen, A., Leaitch, W. R., Lihavainen, H., Mihalopoulos, N., Németh, Z., Nie, W., O'Dowd, C., Salma, I., Sellegri, K., Svenningsson, B., Swietlicki, E., Tunved, P., Ulevicius, V., Vakkari, V., Vana, M., Wiedensohler, A., Wu, Z., Virtanen, A., and Kulmala, M., Global analysis of continental boundary layer new particle formation based on long-term measurements: *Atmos. Chem. Phys.*, 18, 14737-14756, doi:10.5194/acp-18-14737-2018, 2018.

950 Ortega, I. K., Suni, T., Boy, M., Groenholm, T., Manninen, H. E., Nieminen, T., Ehn, M., Junninen, H., Hakola, H., Hellen, H., Valmari, T., Arvela, H., Zegelin, S., Hughes, D., Kitchen, M., Cleugh, H., Worsnop, D. R., Kulmala, M., and Kerminen, V. M., New insights into nocturnal nucleation: *Atmos. Chem. Phys.*, 12, 4297-4312, doi:10.5194/acp-12-4297-2012, 2012.

Pierce, J. R., Leaitch, W. R., Ciggio, J., Westervelt, D. M., Wainwright, C. D., Abbatt, J. P. D., Ahlm, L., Al-Basheer, W., Cziczo, D. J., Hayden, K. L., Lee, A. K. Y., Li, S. M., Russell, L. M., Sjostedt, S. J., Strawbridge, K. B., Travis, M., Vlasenko, A., Wentzell, J. J. B., Wiebe, H. A., Wong, J. P. S., and Macdonald, A. M., Nucleation and condensational growth to CCN sizes during a sustained pristine biogenic SOA event in a forested mountain valley: *Atmos. Chem. Phys.*, 12, 3147-3163, doi:10.5194/acp-12-3147-2012, 2012.

960 Pierce, J. R., Westervelt, D. M., Atwood, S. A., Barnes, E. A., and Leaitch, W. R., New-particle formation, growth and climate-relevant particle production in Egbert, Canada: analysis from

1 year of size-distribution observations: *Atmos. Chem. Phys.*, 14, 8647-8663, doi:10.5194/acp-14-8647-2014, 2014.

Riccobono, F., Schobesberger, S., Scott, C. E., Dommen, J., Ortega, I. K., Rondo, L., Almeida, J., Amorim, A., Bianchi, F., Breitenlechner, M., David, A., Downard, A., Dunne, E. M., Duplissy, J., Ehrhart, S., Flagan, R. C., Franchin, A., Hansel, A., Junninen, H., Kajos, M., Keskinen, H., Kupc, A., Kürten, A., Kvashin, A. N., Laaksonen, A., Lehtipalo, K., Makhmutov, V., Mathot, S., Nieminen, T., Onnela, A., Petäjä, T., Praplan, A. P., Santos, F. D., Schallhart, S., Seinfeld, J. H., Sipilä, M., Spracklen, D. V., Stozhkov, Y., Stratmann, F., Tomé, A., Tsagkogeorgas, G., Vaattovaara, P., Viisanen, Y., Vrtala, A., Wagner, P. E., Weingartner, E., Wex, H., Wimmer, D., Carslaw, K. S., Curtius, J., Donahue, N. M., Kirkby, J., Kulmala, M., Worsnop, D. R., and Baltensperger, U., Oxidation products of biogenic emissions contribute to nucleation of atmospheric particles: *Science*, 344, 717-721, doi:10.1126/science.1243527, 2014.

Riipinen, I., Yli-Juuti, T., Pierce, J. R., Petaja, T., Worsnop, D. R., Kulmala, M., and Donahue, N. M., The contribution of organics to atmospheric nanoparticle growth: *Nature Geoscience*, 5, 453-458, doi:10.1038/ngeo1499, 2012.

Rizzo, L. V., Roldin, P., Brito, J., Backman, J., Swietlicki, E., Krejci, R., Tunved, P., Petäjä, T., Kulmala, M., and Artaxo, P., Multi-year statistical and modeling analysis of submicrometer aerosol number size distributions at a rain forest site in Amazonia: *Atmos. Chem. Phys.*, 18, 10255-10274, doi:10.5194/acp-18-10255-2018, 2018.

Rolph, G., Stein, A., and Stunder, B., Real-time Environmental Applications and Display sYstem: READY: *Environmental Modelling & Software*, 95, 210-228, doi:10.1016/j.envsoft.2017.06.025, 2017.

Rose, C., Sellegrì, K., Velarde, F., Moreno, I., Ramonet, M., Weinhold, K., Krejci, R., Ginot, P., Andrade, M., Wiedensohler, A., and Laj, P., Frequent nucleation events at the high altitude station of Chacaltaya (5240 m a.s.l.), Bolivia: *Atmospheric Environment*, 102, 18-29, doi:10.1016/j.atmosenv.2014.11.015, 2015.

Rose, C., Zha, Q., Dada, L., Yan, C., Lehtipalo, K., Junninen, H., Mazon, S. B., Jokinen, T., Sarnela, N., Sipilä, M., Petaja, T., Kerminen, V.-M., Bianchi, F., and Kulmala, M., Observations of biogenic ion-induced cluster formation in the atmosphere: *Science Advances*, 4, eaar5218, doi:10.1126/sciadv.aar5218, 2018.

Rosenfeld, D., Lohmann, U., Raga, G. B., O'Dowd, C. D., Kulmala, M., Fuzzi, S., Reissell, A., and Andreae, M. O., Flood or drought: How do aerosols affect precipitation?: *Science*, 321, 1309-1313, 2008.

Schobesberger, S., Junninen, H., Bianchi, F., Lönn, G., Ehn, M., Lehtipalo, K., Dommen, J., Ehrhart, S., Ortega, I. K., Franchin, A., Nieminen, T., Riccobono, F., Hutterli, M., Duplissy, J., Almeida, J., Amorim, A., Breitenlechner, M., Downard, A. J., Dunne, E. M., Flagan, R. C., Kajos, M., Keskinen, H., Kirkby, J., Kupc, A., Kürten, A., Kurtén, T., Laaksonen, A., Mathot, S., Onnela, A., Praplan, A. P., Rondo, L., Santos, F. D., Schallhart, S., Schnitzhofer, R., Sipilä, M., Tomé, A., Tsagkogeorgas, G., Vehkamäki, H., Wimmer, D., Baltensperger, U., Carslaw, K. S., Curtius, J., Hansel, A., Petäjä, T., Kulmala, M., Donahue, N. M., and Worsnop, D. R., Molecular understanding of atmospheric particle formation from sulfuric acid and large oxidized organic molecules: *Proc. Natl. Acad. Sci.*, 110, 17,223-17,228, doi:10.1073/pnas.1306973110, 2013.

Seinfeld, J. H., Bretherton, C., Carslaw, K. S., Coe, H., DeMott, P. J., Dunlea, E. J., Feingold, G., Ghan, S., Guenther, A. B., Kahn, R., Kraucunas, I., Kreidenweis, S. M., Molina, M. J., Nenes, A., Penner, J. E., Prather, K. A., Ramanathan, V., Ramaswamy, V., Rasch, P. J., Ravishankara, A. R., Rosenfeld, D., Stephens, G., and Wood, R., Improving our fundamental understanding of the role of aerosol-cloud interactions in the climate system: *Proc. Natl. Acad. Sci.*, 113, 5781-5790, doi:10.1073/pnas.1514043113, 2016.

Simon, M., Dada, L., Heinritzi, M., Scholz, W., Stolzenburg, D., Fischer, L., Wagner, A. C., Kürten, A., Rörup, B., He, X. C., Almeida, J., Baalbaki, R., Baccarini, A., Bauer, P. S., Beck, L., Bergen, A., Bianchi, F., Bräkling, S., Brilke, S., Caudillo, L., Chen, D., Chu, B., Dias, A., Draper, D. C., Duplissy, J., El-Haddad, I., Finkenzeller, H., Frege, C., Gonzalez-Carracedo, L., Gordon, H., Granzin, M., Hakala, J., Hofbauer, V., Hoyle, C. R., Kim, C., Kong, W., Lamkaddam, H., Lee, C. P., Lehtipalo, K., Leiminger, M., Mai, H., Manninen, H. E., Marie, G., Marten, R., Mentler, B., Molteni, U., Nichman, L., Nie, W., Ojdanic, A., Onnela, A., Partoll, E., Petäjä, T., Pfeifer, J., Philippov, M., Quéléver, L. L. J., Ranjithkumar, A., Rissanen, M. P., Schallhart, S., Schobesberger, S., Schuchmann, S., Shen, J., Sipilä, M., Steiner, G., Stozhkov, Y., Tauber, C., Tham, Y. J., Tomé, A. R., Vazquez-Pufleau, M., Vogel, A. L., Wagner, R., Wang, M., Wang, D. S., Wang, Y., Weber, S. K., Wu, Y., Xiao, M., Yan,

C., Ye, P., Ye, Q., Zauner-Wieczorek, M., Zhou, X., Baltensperger, U., Dommen, J., Flagan, R. C., Hansel, A., Kulmala, M., Volkamer, R., Winkler, P. M., Worsnop, D. R., Donahue, N. M., Kirkby, J., and Curtius, J., Molecular understanding of new-particle formation from α -pinene between -50 and $+25$ °C: *Atmos. Chem. Phys.*, 20, 9183-9207, doi:10.5194/acp-20-9183-2020, 2020.

1030

Sipilä, M., Berndt, T., Petäjä, T., Brus, D., Vanhanen, J., Stratmann, F., Patokoski, J., Mauldin, L., Hyvärinen, A.-P., Lihavainen, H., and Kulmala, M., The role of sulfuric acid in atmospheric nucleation: *Science*, 327, 1243-1246, 2010.

1035

Sipilä, M., Sarnela, N., Jokinen, T., Henschel, H., Junninen, H., Kontkanen, J., Richters, S., Kangasluoma, J., Franchin, A., Peräkylä, O., Rissanen, M. P., Ehn, M., Vehkamäki, H., Kurten, T., Berndt, T., Petäjä, T., Worsnop, D., Ceburnis, D., Kerminen, V. M., Kulmala, M., and O'Dowd, C., Molecular-scale evidence of aerosol particle formation via sequential addition of HIO₃: *Nature*, 537, 532-534, doi:10.1038/nature19314, 2016.

1040

Sogacheva, L., Dal Maso, M., Kerminen, V. M., and Kulmala, M., Probability of nucleation events and aerosol particle concentration in different air mass types arriving at Hyytiälä southern Finland, based on back trajectories analysis: *Boreal Environment Research*, 10, 479-491, 2005.

1045

Stein, A. F., Draxler, R. R., Rolph, G. D., Stunder, B. J. B., Cohen, M. D., and Ngan, F., NOAA's HYSPLIT atmospheric transport and dispersion modeling system: *Bull. Am. Meteorol. Soc.*, 96, 2059-2077, doi:10.1175/BAMS-D-14-00110.1, 2015.

1050

Sulo, J., Sarnela, N., Kontkanen, J., Ahonen, L., Paasonen, P., Laurila, T., Jokinen, T., Kangasluoma, J., Junninen, H., Sipilä, M., Petäjä, T., Kulmala, M., and Lehtipalo, K., Long-term measurement of sub-nm particles and their precursor gases in the boreal forest: *Atmos. Chem. Phys.*, 21, 695-715, doi:10.5194/acp-21-695-2021, 2021.

1055

Suni, T., Kulmala, M., Hirsikko, A., Bergman, T., Laakso, L., Aalto, P. P., Leuning, R., Cleugh, H., Zegelin, S., Hughes, D., van Gorsel, E., Kitchen, M., Vana, M., Horrak, U., Mirme, S., Mirme, A., Sevanto, S., Twining, J., and Tardos, C., Formation and characteristics of ions and charged aerosol particles in a native Australian Eucalypt forest: *Atmos. Chem. Phys.*, 8, 129-139, doi:10.5194/acp-8-129-2008, 2008.

1060

Svenningsson, B., Arneth, A., Hayward, S., Holst, T., Massling, A., Swietlicki, E., Hirsikko, A., Junninen, H., Riipinen, I., Vana, M., Dal Maso, M., Hussein, T., and Kulmala, M., Aerosol particle formation events and analysis of high growth rates observed above a subarctic wetland-forest mosaic: *Tellus B*, 60, 353-364, doi:10.1111/j.1600-0889.2008.00351.x, 2008.

1065

Tröstl, J., Chuang, W. K., Gordon, H., Heinritzi, M., Yan, C., Molteni, U., Ahlm, L., Frege, C., Bianchi, F., Wagner, R., Simon, M., Lehtipalo, K., Williamson, C., Craven, J. S., Duplissy, J., Adamov, A., Almeida, J., Bernhammer, A.-K., Breitenlechner, M., Brilke, S., Dias, A., Ehrhart, S., Flagan, R. C., Franchin, A., Fuchs, C., Guida, R., Gysel, M., Hansel, A., Hoyle, C. R., Jokinen, T., Junninen, H., Kangasluoma, J., Keskinen, H., Kim, J., Krapf, M., Kürten, A., Laaksonen, A., Lawler, M., Leiminger, M., Mathot, S., Möhler, O., Nieminen, T., Onnela, A., Petäjä, T., Piel, F. M., Miettinen, P., Rissanen, M. P., Rondo, L., Sarnela, N., Schobesberger, S., Sengupta, K., Sipilä, M., Smith, J. N., Steiner, G., Tomè, A., Virtanen, A., Wagner, A. C., Weingartner, E., Wimmer, D., Winkler, P. M., Ye, P., Carslaw, K. S., Curtius, J., Dommen, J., Kirkby, J., Kulmala, M., Riipinen, I., Worsnop, D. R., Donahue, N. M., and Baltensperger, U., The role of low-volatility organic compounds in initial particle growth in the atmosphere: *Nature*, 533, 527-531, doi:10.1038/nature18271, 2016.

1070

Twomey, S. A., Piepgrass, M., and Wolfe, T. L., An assessment of the impact of pollution on global cloud albedo: *Tellus*, 36B, 356-366, 1984.

1075

Uusitalo, H., Kontkanen, J., Ylivinkka, I., Ezhova, E., Demakova, A., Arshinov, M., Belan, B. D., Davydov, D., Ma, N., Petäjä, T., Wiedensohler, A., Kulmala, M., and Nieminen, T., Occurrence of new particle formation events in Siberian and Finnish boreal forest: *Atmos. Chem. Phys. Discuss.*, doi:10.5194/acp-2021-530, 2021.

1080

Vehkamäki, H., Dal Maso, M., Hussein, T., Flanagan, R., Hyvärinen, A., Lauros, J., Merikanto, J., Mönkkönen, P., Pihlatie, M., Salminen, K., Sogacheva, L., Thum, T., Ruuskanen, T. M., Keronen, P., Aalto, P. P., Hari, P., Lehtinen, K. E. J., Rannik, Ü., and Kulmala, M., Atmospheric particle formation events at Värriö measurement station in Finnish Lapland 1998-2002: *Atmos. Chem. Phys.*, 4, 2015-2023, doi:10.5194/acp-4-2015-2004, 2004.

1085

Vo, E., Horvatin, M., and Zhuang, Z. Q., Performance comparison of field portable instruments to the scanning mobility particle sizer using monodispersed and polydispersed sodium chloride aerosols: *Annals of Work Exposures and Health*, 62, 711-720, doi:10.1093/annweh/wxy036, 2018.

- Wang, M., and Penner, J. E., Aerosol indirect forcing in a global model with particle nucleation: *Atmos. Chem. Phys.*, 9, 239-260, doi:10.5194/acp-9-239-2009, 2009.
- Wiedensohler, A., Ma, N., Birmili, W., Heintzenberg, J., Ditas, F., Andreae, M. O., and Panov, A., Infrequent new particle formation over the remote boreal forest of Siberia: *Atmospheric Environment*, 200, 167-169, doi:doi.org/10.1016/j.atmosenv.2018.12.013, 2019.
- 1090 Wimmer, D., Buenrostro Mazon, S., Manninen, H. E., Kangasluoma, J., Franchin, A., Nieminen, T., Backman, J., Wang, J., Kuang, C., Krejci, R., Brito, J., Goncalves Morais, F., Martin, S. T., Artaxo, P., Kulmala, M., Kerminen, V. M., and Petäjä, T., Ground-based observation of clusters and nucleation-mode particles in the Amazon: *Atmos. Chem. Phys.*, 18, 13245-13264, doi:10.5194/acp-18-13245-2018, 2018.
- 1095 Yan, C., Yin, R. J., Lu, Y. Q., Dada, L. N., Yang, D. S., Fu, Y. Y., Kontkanen, J., Deng, C. J., Garmash, O., Ruan, J. X., Baalbaki, R., Schervish, M., Cai, R. L., Bloss, M., Chan, T., Chen, T. Z., Chen, Q., Chen, X. M., Chen, Y., Chu, B. W., Dallenbach, K., Foreback, B., He, X. C., Heikkinen, L., Jokinen, T., Junninen, H., Kangasluoma, J., Kokkonen, T., Kurppa, M., Lehtipalo, K., Li, H. Y., Li, H., Li, X. X., Liu, Y. L., Ma, Q. X., Paasonen, P., Rantala, P., Pileci, R. E., Rusanen, A., Sarnela, N., Simonen, P., Wang, S. X., Wang, W. G., Wang, Y. H., Xue, M., Yang, G., Yao, L., Zhou, Y., Kujansuu, J., Petaja, T., Nie, W., Ma, Y., Ge, M. F., He, H., Donahue, N. M., Worsnop, D. R., Kerminen, V. M., Wang, L., Liu, Y. C., Zheng, J., Kulma, M., Jiang, J. K., and Bianchi, F., The synergistic role of sulfuric acid, bases, and oxidized organics governing new-particle formation in Beijing: *Geophys. Res. Lett.*, 48, e2020GL091944, doi:10.1029/2020gl091944, 2021.
- 1100 Yu, F., and Luo, G., Simulation of particle size distribution with a global aerosol model: contribution of nucleation to aerosol and CCN number concentrations: *Atmos. Chem. Phys.*, 9, 7691-7710, 2009.
- 1105 Yu, H., Ortega, J., Smith, J. N., Guenther, A. B., Kanawade, V. P., You, Y., Liu, Y., Hosman, K., Karl, T., Seco, R., Geron, C., Pallardy, S. G., Gu, L., Mikkila, J., and Lee, S.-H., New particle formation and growth in an isoprene-dominated Ozark forest: From sub-5 nm to CCN-active sizes: *Aerosol Sci. Tech.*, 48, 1285-1298, doi:10.1080/02786826.2014.984801, 2014.
- 1110 Zhang, R. Y., Khalizov, A., Wang, L., Hu, M., and Xu, W., Nucleation and growth of nanoparticles in the atmosphere: *Chem. Rev.*, 112, 1957-2011, doi:10.1021/cr2001756, 2012.
- 1115 Zheng, G., Wang, Y., Wood, R., Jensen, M. P., Kuang, C., McCoy, I. L., Matthews, A., Mei, F., Tomlinson, J. M., Shilling, J. E., Zawadowicz, M. A., Crosbie, E., Moore, R., Ziemba, L., Andreae, M. O., and Wang, J., New particle formation in the remote marine boundary layer: *Nature Communications*, 12, doi:10.1038/s41467-020-20773-1, 2021.
- 1120 Zhu, J., and Penner, J. E., Global modeling of secondary organic aerosol with organic nucleation: *J. Geophys. Res.*, 124, 8260-8286, doi:10.1029/2019JD030414, 2019.